Shear Behavior of HSC Beams Reinforced with Steel and Fiber Composite Grids

A Thesis

Presented in Partial Fulfillment of the Requirements for the

Master of Science in Civil Engineering

in the

College of Graduate Studies

University of Idaho

by

Mohammad Azhar Mudaqiq

Major Professor: Ahmed Ibrahim, Ph.D.

Committee Members: Richard Neilson, Ph.D., Ahmed Abdel–Rahim, Ph.D.

Department Administrator: Patricia Colberg, Ph.D.

May 2018

Authorization to Submit Thesis

This thesis of Mohammad Azhar Mudaqiq, submitted for the Master of Science in Civil Engineering and titled **"Shear Behavior of HSC Beams Reinforced with Steel and Fiber Composite Grids"** has been reviewed in the final form. Permission, as indicated by the signature and dates below, is now granted to submit final copies to the college of Graduate studies for approval.

Major Professors:

_____ Date: _____

Ahmed Ibrahim, Ph.D.

Committee Members:

_____ Date: _____

Richard Neilson, Ph.D.

_____ Date: _____

Ahmed Abdel-Rahim, Ph.D.

Department Administrator:

_____ Date: _____

Patricia Colberg, Ph.D.

Abstract

Fiber reinforced polymer (FRP) grids are commercially known as NEFMAC. It has been used in various applications such as bridge decks. Very limited research is available on the contribution of the FRP grids to concrete shear strength and the feasibility of using the design codes in quantifying moment capacity and shear strength of High Strength Concrete beams. This study investigates the shear behavior of High Strength Concrete beams strengthened with conventional and FRP grid together acting as a hybrid reinforcement system. NEFMAC is composed of continuous high-strength reinforcing fibers inserted in a vinyl ester resin. The FRP laminate are shaped into 2 dimensional grid using layering process. In order to satisfy the 2-D geometric and mechanical properties, the longitudinal and transverse bars are continuous at the point of intersection. The FRP reinforcement grids are rectangular with smooth top and bottom surfaces. Six High Strength Concrete beams were prepared and tested under four-point monotonic load with various shear span-to-depth ratios (2.0 and 2.5). All beams have a 7 foot span with 6 x 12 inches cross sections. The beams are designed and reinforced with conventional steel bars and carbon fiber reinforced polymer (CFRP) 2-D grids. All beams are designed to have a dominant shear failure. Some beams are designed to have both traditional steel and the CFRP grid as reinforcement to show potential advantages using a combination of hybrid reinforcement. The main key parameters are the shear span-to-depth ratio, and the reinforcement type (conventional steel, CFRP grids, and hybrid fibers). Strain gages were placed internally on the CFRP grid and externally on the concrete compression surface to properly measure the induced stresses. Load-deflection behavior and flexural strain is presented to model the beams ultimate loads and deflections obtained during the monotonic loading. The test results showed the potential advantages of using CFRP grids in RC beams in

terms of increasing the beams ductility and load-carrying capacity. The shear and flexural stiffness were compared for different beam groups and the effective force transfer mechanisms of the 2-D grids were presented.

Keywords: Reinforced Concrete, High Strength Concrete, Carbon Fiber Grids, Deflection, Effective Moment of Inertia

Acknowledgments

In the name of God, the most merciful and compassionate.

I would like to wholeheartedly thank Dr. Ibrahim for serving as the chairman of my committee. His inspiring words of wisdom have opened the door of knowledge and have been a principle reason for my eagerness to continue on this path. His caring thoughts have brightened the road of education and research for me.

I would also like to thank Nick Saras, Abullah Almakrab, Don Parks, Niyi Arowojolu, Ahmed Arafat and Moustapha Amadou for their constant help and support in conducting the thesis experiments. A special gratitude goes to Sarah Aranguiz (Memo) for her words of encouragement and constant support. This experiment would not have been done without their tireless efforts and tedious work.

Acknowledgemet of Jesse Espy, manager of Pre-Mix Inc., for his generous donation of the concrete mixtures needed to accomplish the work done in this thesis as well as the Department of Civil and Environmental Engineering at the University of Idaho for the support given to this research through its facilities and for granting me the opportunity to pursue my graduate studies.

Dedication

I am dedicating my thesis to my beloved parents:

Mohammad Amin Mudaqiq and Khadija Mudaqiq

Table of Content

List of Figures

List of Tables

Notations

ST = Steel

GF = GFRP

CF = CFRP

MN = Monotonic load

2 = Shear span of 2

2. 5 = Shear span of 2. 5

M_x = Moment capacity obtained by the applied load

P = Load applied to the RC beam

ε_t = Strain of the reinforcement collected by the strain gages

$\emptyset$ = Shows the curvature of the section

a = Shear span of reinforced concrete beam

$M_{u\,(frp)}$ = Ultimate moment of FRP reinforcement

$M_{u\,(steel)}$ = Ultimate moment of steel reinforcement

$\emptyset_{frp}$ = Material resistance factor of FRP reinforcement

f_{frpu} = Ultimate tensile strength of FRP reinforcement

f_{steelu} = Ultimate tensile strength of grade 60 steel reinforcement

β = Stress – block parameter for concrete at a strain less than ultimate

c = Depth of neutral axis

$\rho_{\,balance\,(frp)}$ = Balanced failure reinforcement ratio

ρ_w = Reinforcement ratio

f_y = Steel tensile strength

E_{frpu} = Elastic Modulus of FRP

f'_c = Concrete strength

b_w = Width of the concrete beam

d = Effective depth of the concrete section

V_c = The shear strength provided by the concrete

V_s = The shear strength provided by the stirrups

$f'c$ = The compressive strength of the concrete

b_w = The width of the web

ρ_w = Longitudinal reinforcement ratio

V_u = Shear force

M_u= The ultimate Moment

λ = Lightweight concrete modification factor

I_t = Moment of Inertia at transformed section

I_{cr} = Moment of Inertia of the cracked section transformed to concrete with concrete in tension is ignored

M_{cr} = Cracking moment of cross section

M_a = Maximum moment in a member of at the load stage at which deflection is being calculated

b = Width of the concrete

h = Overall member depth

k = Neutral axis factor or ratio of the position of the neutral axis to the effective depth used in linear elastic stress analysis

n = Modular ratio

f_r = Modulus of rupture

y_t = Distance from the neutral axis to the bottom of the beam where tensile stress is maximum

Δ_{Max} = Maximum Deflection

P = Maximum applied load

E_c = Effective Modulus of elasticity of concrete

I_e = Effective moment of inertia

l = Length of the concrete beam

CHAPTER 1: INTRODUCTION

1.1 PROBLEM STATEMENT:

The conventional reinforcing bar also known as the normal steel rebar has been used as reinforcing material in concrete structures and industries since the 15th century. These hot rolled reinforcing bars are widely used as tensioning material in order to hold concrete in a compressed state. A basic understanding of concrete indicates that concrete is very weak in tension but extremely strong in compression; thus, steel reinforcement is used to hold concrete in tension and strengthen concrete structures. Concrete buildings that are internally reinforced with reinforcing steel bars last about 100 years and are considered to be cost effective and have increased ductility and durability. Not only are steel bars an excellent material that offers a stylish method of building gigantic concrete structures, but they also allow structural designers the freedom to explore more design options for generating modern floor plans. One of the main problems that engineers face with concrete buildings is corrosion. Recent studies show that 90 percent of the damage in structures is caused by corrosion of reinforcing steel. Corrosion is accelerating the critical age of concrete and shortening the structures service life. Billions of dollars are spent annually for maintenance of concrete structures deteriorated due to corrosion. As a result, engineers have been looking for other reinforcing materials to replace normal reinforcing steel bars. Fiber Reinforced Polymer (FRP) is one of the latest and newest materials being used as a replacement for conventional steel reinforcement due to its advantages: high strength, non-conductive, lightweight, low thermal conductivity, impact resistant and most importantly, high corrosion resistance. FRP bars are also linearly elastic and which can lead to a brittle failure with no advanced warning. One the key disadvantages of FRP bars are its lower modulus of elasticity which creates

larger cracks and deflections. One of the products of the fiber composites is the FRP grids, which are commercially known as NEFMAC. It has been used in various applications, like bridge decks for example. FRP grids consist of Glass Fiber Reinforced Polymer (GFRP) and or Carbon Fiber Reinforced Polymer (CFRP). Limited research is reported about the shear behavior of the FRP grids in High Strength Concrete (HSC) beams. This thesis presents the results of testing 6 HSC beams reinforced with hybrid reinforcement (steel plus glass or carbon FRP grids). The results present the load-deflection, load-strain, ultimate load, failure displacement, and the mode of failure of all beams. The results were compared with the prediction equations of the Canadian code of beams reinforced with FRP bars to investigate its feasibility for HSC beams reinforced with hybrid fibers.

1.2 OBJECTIVE OF RESEARCH

The main objectives for this study:

- Investigate shear behavior of High Strength Concrete beams reinforced with fiber composite grids coupled with reinforcing steel as a hybrid reinforcing system.
- Understand the behavior of HSC concrete under monotonic load and the corresponding mode of failure and cracking pattern of the beams.
- Test the feasibility of the Canadian code for predicting deflection, maximum load, effective moment of inertia, ultimate moment and cracking moment capacity for the HSC hybrid beams.

The process has been achieved by casting 6 concrete beams with different reinforcements of steel with GFRP or CFRP grid. The Pre-Mix Inc. generously provided the HSC concrete that possess the compressive strength of 9,000 psi. All beams were cured for 28 days under wet towels. The 6 beams were designed to fail in shear, more properly known as diagonal tension

failure, which is still not well understood despite many years of research and investigation. If a concrete beam is overloaded without properly being designed for shear reinforcement, the shear failure will occur suddenly, and it will cause severe damage to the concrete structures. Any concrete members with no shear reinforcement will fail immediately upon the formation of initial crack with the applied load. Thus, the 6 hybrid concrete beams will be analyzed for shear strength, deformation, flexural strength, crack width, and distance between the cracks.

1.1 THESIS OUTLINE

This thesis is mainly divided into two parts: the first part (Chapter 2 to 3) provides information about the beams, its experimental design and previous research, and the second part (chapter 4 and 5) which discuss, evaluate, and analyze the results obtained from the casted beams.

Chapter 2: "INTRODUCTION TO FRP GRID": This chapter talks about the introduction and background of FRP grid.

Chapter 3: "LITERATURE REVIEW FOR FRP GRID": This chapter summarizes any existing and relevant previous research done in the similar area of research and investigated CFRP, GFRP, steel and hybrid as beam reinforcement using Ultra High Strength Concrete.

Chapter 4: "EXPERIMENTAL DESIGN AND METHOD FOR FRP GRID": This chapter covers and describes the experimental plan and setup for the casted 5 beams and discusses every step of the experiment and its measurements as well as testing procedures.

Chapter 5: "RESULT AND DISCUSSIONS FOR FRP GRID": This chapter analyzes the obtained test results from the concrete beams reinforced either with hybrid of steel with GFRP or CFRP.

Chapter 6: “SUMMARY AND CONCLUSION”: This chapter reveals the conclusion of the casted beams and compare the result with the previously 9 casted concrete beams. It also includes recommendations for future researchers who would like to conduct research with FRP concrete beams.

CHAPTER 2: INTRODUCTION TO FRP GRID

2.1 GENERAL

Fiber reinforced polymers (FRP) has been a desirable nonmetallic reinforcement for concrete buildings due to its essential and important properties. The significance of FRP properties range from being nonconductive to lightweight, non-magnetic, corrosion resistant, low density, and most importantly high tensile strength. FRP is mainly a composite material that is reinforced with fiber and the fiber used in the FRP is usually carbon, glass, or aramid. Composite materials are normally made of two or more basic materials that have different chemical or physical traits and combining these two materials together creates a unique and strong materials with lower density. FRP are used as reinforcement in aggressive environments such as chemical plants, marine environments, or other buildings/bridges being exposed to harmful chemical materials like salt, sulfur, chloride, etc.

The most commonly used FRP contains glass or carbon and they are used as reinforcement for normal concrete structures. Due to its anti-corrosion properties, engineers are looking to replace normal steel bars with FRP reinforcement to extend the age of the concrete structures and avoid the cost of maintenance that is caused by corrosion. However, FRP have lower modulus of elasticity and have a linear elastic response until the initial crack occurs under the certain applied load. FRP is considered to have poor resistance to high temperatures and fire. They are also expensive compare to conventional steel bars and are weak in bending when exposed to the high capacity of applied load. From a structural engineering point of view, FRP in transverse direction has a significantly lower shear strength and lacks plastic behavior when used as reinforcements [1].

2.2 FIBER REINFORCED POLYMER HYBRID WITH STEEL

Engineers have been using steel for reinforcement of concrete structures for decades, and still remains as a popular choice for reinforced concrete structures. Steel and concrete both have the same thermal expansion for extensively high temperature. Steel has excellent bending properties and tension strength to withstand the applied load. Steel is also known for its excellent ductility property to withstand any sort of impact or cyclic load and compared to FRP, it plays an important role. FRP has lower linear elastic behavior and thus a lot has been done to extend the value of ductility of FRP. The lightweight, fatigue durability, and transparency of FRP bars to electric and magnetic fields are making FRP an excellent substitution to steel reinforcement [2].

Carbon Fiber Reinforced Polymer (CFRP) has higher tensile strength and excellent elastic modulus which is similar to normal steel. Its strength to weight ratio is the highest compared to other FRPs in the industry. Combining CFRP with steel bars shows significant increase in the breaking strain and such increases is strongly depended on the adhesion between steel and CFRP [3]. Glass Fiber Reinforce Poly (GFRP) have higher heat resistance properties and also have a unique behavior of being high in electrical insulating compared to other FRPs. One of the main weaknesses of GFRP is its lower resistance to sudden impact applied load which is due to the lack of plastic deformation that cannot absorb the impact energy. A combination of steel with GFRP increases the ductility, stiffness, and load resistance after the initial crack. The amount of CFRP and steel usage in the concrete beams needed to be taken into consideration. With a greater amount of GFRP reinforcement, it will decrease the rate of ultimate moment of capacity and lower the beam strength. The hybrid of GFRP and steel

significantly decreases the stiffness, but will increase the deflection of the beam after the initial crack and yield of the steel reinforcement is reached [4].

CHAPTER 3: LITERATURE REVIEW

3.1 INTRODUCTION

Development of Fiber Reinforced Polymers (FRPs) have changed the dynamic of concrete structures. Engineers consider FRPs one of the best substitutes of normal steel bars used as longitudinal reinforcements in concrete beams. FRPs are unique composite materials that possess a vast range of important mechanical and physical behaviors compared to other metal steel bars. FRPs are corrosion free with high tensile strength and can deliver more strength per unit of its weight than most metals [5]. Steel rebars also have a proven history as concrete reinforcement since at least 15^{th} century. Compared to FRPs, they are cost-effective and have sufficient tensile strength to support concrete structures. FRPs also behave differently from steel when it comes to linear elastic behavior until failure. The final failure of FRP reinforced concrete beams are usually brittle and sudden with no warning in the form of notable deformation [6]. Based on the previous research, combination of steel bars and FRP has shown significant increases in the strength, serviceability and durability of concrete beams. Due to linear elastic behavior of FRP, the ductility and strength strictly depends on the amount of FRP and steel because the deformation behavior of hybrid (steel + FRP) beams are different than concrete that are only reinforced with FRP or conventional steel rebar [7]. Hybrid beam is defined as a beam that contains steel and FRP as main reinforcement. The reinforcing beams with steel and FRP have mutual benefits of completing each other's flaws and weaknesses. Steel bars are more exposed to corrosion while FRP bars have the advantage of corrosion resistance behavior. An optimal solution can be achieved when placing FRP bars in the extreme tensile zone with small concrete cover thickness and the steel bars placed on the top of the FRP layer with a larger concrete cover [8]. This will lead to the achievement of

better corrosion resistance member with reasonable strength and ductility. To further understand the concept of hybrid concrete beams, the up-to-date research has been collected and cited as in the following sections. The shear and flexural behavior of reinforced concrete beams with FRP or FRP hybrid with steel rebar will be discussed as follows.

3.2 BEHAVIOR OF BEAMS REINFORCED WITH FRP

Recently, CFRP materials are attracting interest for their potential as a high strength, durable replacement steel of the reinforcement in concrete members. Various studies have been investigating the effects of fiber polymers in concrete members, which is leading to promising results.

Wenjun Qu et al, explored the flexural behavior of concrete beams reinforced with hybrid reinforcement that mainly consisted of GFRP and steel rebar. During the experimental and theoretical investigation, eight beams including two control beams reinforced with only steel (B1) or GFRP (B2) and 6 other beams reinforced with mix of steel and GFRP were casted to examine the strength, durability, and serviceability of the new reinforcing techniques. The dimensions of all beams were 180 X 250 X 1800 mm. The Table 3.1 shows the details of the casted concrete beams.

Table 3.1: Details of casted and tested beams (11)

Details of Tested Beams

Beam number	$A_s\,(\mathrm{mm}^2)$	$A_f\,(\mathrm{mm}^2)$	$A\,(\mathrm{mm}^2)$	R_f	ρ_{eff} (%)	$\rho_{\mathrm{eff},b}$ (%)	f_{cu} (MPa)
B1	452.16	–	452.16	0	1.14	3.23	30.95
B2	–	506.45	506.45	–	0.29	–	30.95
B3	226.08	253.23	479.31	0.252	0.71	3.45	33.10
B4	200.96	396.91	597.87	0.405	0.71	3.73	33.10
B5	401.92	141.69	543.61	0.066	1.08	3.88	34.40
B6	401.92	253.23	655.15	0.142	1.16	3.88	34.40
B7	113.04	141.69	254.73	0.236	0.35	4.08	40.65
B8	1,205.76	396.91	1,602.67	0.067	3.49	4.41	40.65

During the testing, loads were gradually applied with a hydraulic jack and at every load level crack initiation and propagation were examined as well as beam strain, deflection, and load history. As a result of the experiment, hybrid beams reinforced with normal steel showed good ductility and load carry capacity and they were all failed due to crashing of concrete in the compressive area after the steel bars yielded. However, the stress level of the GFRP reached a small percentage of its ultimate value. At the end of linear phase, beams began to crack and the stiffness decreased after cracking. Table 3.2 shows the result details of the study.

Table 3.2: Maximum loads and failure modes (11)

Beam number	P_{exp} (kN)	P_{th} (kN)	P_{th}/P_{exp}	P_{de} (kN)	P_{de}/P_{exp}	Failure mode
B1	107.9	108.9	1.009	105.8	0.981	Steel yielding, concrete crushing
B2	146.3	136.9	0.936	128.3	0.877	Concrete crushing
B3	127.6	134.8	1.056	126.5	0.991	Steel yielding, concrete crushing
B4	132.2	145.4	1.100	136.1	1.030	Steel yielding, concrete crushing
B5	121.2	131.3	1.083	124.7	1.029	Steel yielding, concrete crushing
B6	141.9	155.1	1.093	146.0	1.029	Steel yielding, concrete crushing
B7	78.5	83.3	1.061	96.2	1.225	Steel yielding, concrete crushing
B8	211.0	272.8	1.293	233.3	1.106	Steel yielding, concrete crushing

As a conclusion, the authors argued that the flexural behavior of the concrete beams are enhanced with steel reinforcement and GFRP combination and the steel reinforcement also improves the ductility of the hybrid reinforced beams as well as the defection [11].

Sumant U. et al. examined the flexural strength and split tensile strength of concrete beams reinforced with glass fiber polymers. The GFRP is built from continuous fiber filament that is embedded in resin matrix of different types of shapes such as bars, structures sections, plates and fabric. Even though GFRP bar has lowered the elastic modulus, it offered good benefits

of having high tensile strength-to-weight ratio, corrosion-free, lightweight, non-magnetic, and most importantly non-conductive. Sumant U. et al. showed that significant improvement in strength was observed with inclusion of glass fiber in plain concrete and it has revealed that the maximum strength depends upon the amount of fiber content. The researchers have also found significant increases in the flexural strength of concrete with glass fiber polymer and the number of cracks with GFRP is comparatively less than plain concrete [12].

A study that was conducted by Saleh et al. investigated the flexural behavior of 12 concrete beams reinforced with GFRP bars. The study examined the comparison between the measured and predicted load and deflection of all beams that were reinforced either with steel or GFRP bars. The results showed a drop in the load deflection at each time the beam cracks which appears to be because of the low modulus elasticity of the GFRP bars. Before the failure occurred, the strain in the GFRP increased and a larger tensile strength was developed in the reinforcing bars. The result also shows that when the applied load reach 20 KN, the deflection of the group B is almost twice compared to group A beams. In the different reading, it shows that when the applied load on series B is 12 KN, the deflection of the series B is the same as the deflection of series when series A is under the 20 KN applied load. This result shows that replacing the conventional steel bars with GFRP without changing the cross-sectional dimension might not be a practical alternative for the concrete structures. In conclusion, the author claims that using a factor of safety of 1.5 against the possibility of tensile failure of GFRP bars prevent the catastrophic failure and it will assure the gradual failure of FRP-RC due to concrete compression [13]

Shawn P. et.al. studied the shear strength of the normal and high strength concrete beams that are reinforced with glass fiber reinforced polymer with no web reinforcements. 30 concrete beams were poured and tested. 18 beams were casted with normal strength concrete and 12 other beams were casted with High Strength Concrete having GFRP as their longitudinal reinforcement. None of the 30 beams contained web reinforcements and the reinforcement ratios ranged from 1.11% to 2.27% used for normal strength concrete beams and 1.25% to 2.56% for High Strength Concrete beams. Also, 6 complementary steel reinforced beams, 3 with normal strength concrete and the remaining other 3 with High Strength Concrete, were casted and tested to analyze the shear strength. During the beams testing, the failure was sudden and some of the beams sustained most of its load capacity for a while after the failure. Shear cracks occurred during the experiments along the entire width and depth of the section. The authors concluded that longitudinal reinforcement ratio has a minimal effect on the concrete shear strength. High Strength Concrete beams showed slightly less shear strength compare to the normal strength concrete beams. The researchers also claimed that as neutral axis moves closer the extreme compression fiber, the contribution of aggregate interlocking decreases and it would lead to wider cracks in the beam. The nonlinear relationship of neutral axis and reinforcement ratio is responsible for lower shear strength for High Strength Concrete relative to normal strength concrete beams [14].

Another study that investigated the flexural and shear behavior of concrete beams with GFRP in have been reported by Ashour et al. All the twelve beams tested under four-point loading and had no shear or compression reinforcement. Flexure and shear were the two types of

failure observed in the tested concrete beams. The behavior of the failed beams was similar in terms of having initial cracking that were observed at the mid span

Due to the lower modulus of elasticity to tensile strength ratio of GFRP, the cracks in the mid span became wider and more cracks also started showing up when more loads were applied. There were two types of failure that occurred. Flexure failure occurred for the under reinforced beams in the mid span while the over reinforced beams failed in shear in the shear span and the cracks became more inclined and propagated toward the loading point.

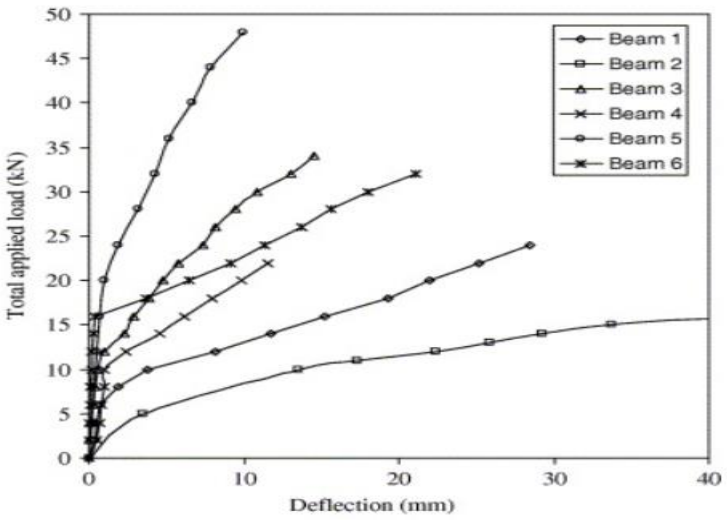

Figure 3.1: Deflection of the 6 beams (15)

Figure 3.1 shows the deflection of the different beams and based on the graph the researchers claim that all beams behaved linearly until the first cracks occurred and the flexural stiffness of the beam changed drastically after the initial crack. Beams that failed in deflection exhibited larger deflection while beams that failed in shear showed lower deflection [15].

D.H. Tavares et.al. studied the behavior and characteristic of concrete beams that are reinforced with GFRP bars. This study analyzed and compared displacement, reinforcement deformation, flexural strength, and bonding between steel and GFRP reinforced beams. Six

concrete beams were casted and tested in the laboratory under four-point loading. GFRP has high strength to weight ratio, high tensile strength, and no conductive properties and their thermal expansion is similar to concrete. The dimensions of the casted beams was 2900 x 150 x 300 mm and 1 of the 6 beams was reinforced with deformed steel bars and the remaining 5 beams were reinforced with GFRP. Figure 3.2 shows the geometry of the concrete beams:

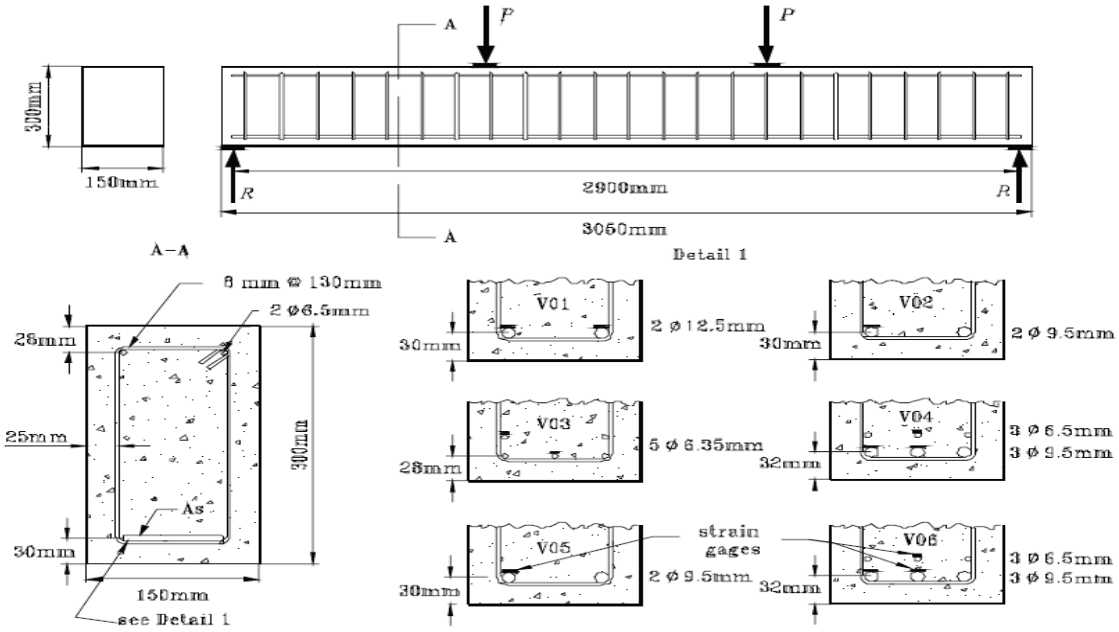

Figure 3.2: Geometry and experimental setup of the concrete beams (16)

Based on the longitudinal tensile strength recorded from strain gages that were placed on the lowest level of reinforcement, it can be said that the flexural failure of the specimen was due to the compressive crushing after the yielding has occurred. Cracks were initiated in the concrete beams at an applied load of 20 kN and then steel reinforcement maintained a linear strain until the yielding happened. The strain obtained in the GFRP was greater than the strain of the steel reinforcement and GFRP also had higher deformation compared to steel.

It was concluded that lower modulus of elasticity and relative higher GFRP rapture strain were the key factors that caused the flexural behavior of the concrete beams reinforced with GFRP

bars. The capacity of GFRP beams with the same internal tension force was lower than the steel reinforced beam with the same internal tension forces [16].

3.4 BEHAVIOR OF HIGH STRENGTH CONCRETE WITH FRP

Yinghao Liu and Yong Yuan conducted a study about the feasibility of High Strength Concrete beams reinforced with steel and GFRP. This study analyzed the flexural behavior of High Strength Concrete beams reinforced with internally and longitudinal GFRP and normal steel bars. The downside to using GFRP was its lower elastic modulus which caused cracks and larger deflection in all beams. Thus, FRP rebar hybrid with normal steel was considered to be effective to tackle these problems. Four concrete beams were casted and tested. One of the beams was only reinforced with GFRP and the remaining three were reinforced with the combination of steel and GFRP rebars. The dimension of the beams were 2000 x 150 x 250 mm and the four beams were labeled as S1, S2, S3, and S4. Table 3.3 shows the details of the beams and the test setup:

Table 3.3: Details of the concrete specimen (20)

Beam	Number of steel rebars	Number of GFRP rebars	[7] $\rho_{eff,b}$ (%)	ρ_{eff} (%)	Beam classification
S1	0	4	0.7	1.2	Over-reinforced
S2	2	2	8.56	2.64	Under-reinforced
S3	2	2	8.56	2.64	Under-reinforced
S4	2	2	8.56	2.64	Under-reinforced

S1 beam was only reinforced with GFRP which revealed more deflection and wider and additional cracks compared to the other specimens due to its lower elastic modulus. The beam also failed abruptly when the maximum load was reached which was also due to its linear elastic property. The strain distribution was different at different levels of the applied loads

and it was almost proportional to the distance from the neutral axis. Table 3.4 shows the flexural capacity of the four beams with the corresponding mode of failure.

Table 3.4: Shows the moment force and failure mode of the concrete beams (20)

Specimens	Theoretical ultimate moment $M_{u,th}$(kNm)	Actual ultimate moment $M_{u,exp}$(kNm)	$M_{u,th}/M_{u,exp}$	Failure mode
S1	81.3	72.5	1.12	Concrete crush
S2	80.3	69.9	1.14	Steel yield, concrete crush
S3	80.3	74.8	1.07	Steel yield, concrete crush
S4	80.3	82.0	0.97	Steel yield, concrete crush

Combing steel bars with GFRP significantly improved the maximum applied load and failure compare to S1 specimen that's only reinforced with GFRP. The impact of applied maximum force is significantly clear for different levels of reinforcement in the flexural strength of the beam and the flexural strength increases as the number of steel bar decreases. Figure 3.3 shows the load deflection curve for all the tested beams.

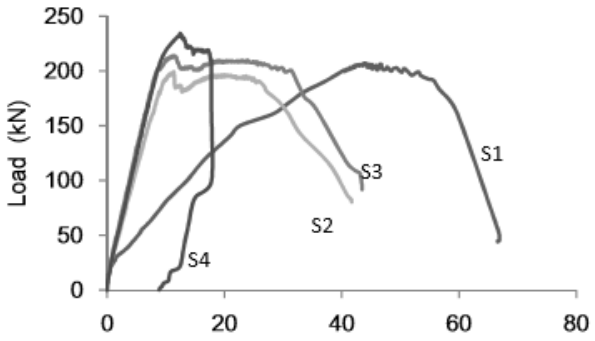

Figure 3.3: Load deflection curve of the beams *(20)*

It can be concluded that the deflection of hybrid beams was significantly impacted by the position of the steel bars. Based on the graph, the deflection of S1 is 4~5 of the deflection of hybrid beams. For the hybrid beams, it can be observed that the deflection is linear until the initial crack and the stiffness of the beams decreases significantly after cracking. The combination of steel and GFRP controls the deflection and increases the flexural strength of

the concrete beams as well as decreases the reinforcements ratio. Hybrid concrete beams also had a stable neutral axis and was not impacted by the applied load [20].

3.5 SHEAR BEHAVIOR OF BEAMS REINFORCED WITH HYBRID REINFORCEMENT

M.S Alam et al. studied the size effect on shear strength of 12 FRP reinforced concrete beams reinforced with no stirrups. The authors claim that concrete beams reinforced with glass FRP bars are low in shear strength compared to concrete beams reinforced with the same amount of steel reinforcement which is due to the low modulus of elasticity and brittle elastic failure of glass FRP bars. Four beams were reinforced with a different type of reinforcement; glass FRP, carbon FRP, and steel bars in the longitudinal directions. ACI-ASCE committee 445 (1998) revealed that reinforced concrete beams with no stirrups can resist the shear by the mean of aggregate interlock, dowel action of longitudinal reinforcement, arch action, and residual tensile stress across the cracks and shear resistance of un-cracked concrete compression zone. This signifies that it can be relatively different when it comes to concrete beams reinforced with FRP which is attributed to lower transverse stiffness and strength of FRP reinforcement. It was concluded that the depth of the beams is proportional to the crack spacing; the wider the cracks, the more reduction of shear strength. When the shear span-to-depth ratio of the beam was equal to 2.5, the mode of failure of the FRP reinforced beams that included shear tension, shear compression, or diagonal tension, was similar to the failure of the beams with normal steel reinforcement. This experiment exhibits that the inverse of the cubic root of the effective depth of the beam is directly proportional to the normalized shear

strength. In other words, shear strength at failure decrease when the member depth of the concrete beam increases for any type of reinforcement [21].

Fabio Matta et.al. investigated the shear strength of five concrete beams that are reinforced with fiber reinforced polymer without stirrups and examined the size effect of the reinforcement on the shear strength. The studies showed that concrete beams reinforced with GFRP had wider flexural cracks compared to normal steel reinforcement in one way member without any kind of reinforcement for shear, which was due to the lower stiffness of GFRP [22].

The CRFPs also have been widely used in eight concrete beams as main reinforcement, Z. Omeman et al. Four control beams and four other beams reinforced with the CFRP bars and no web reinforcements. It was also concluded that CFRP has significant impact on the shear strength and deflection of the short beams when they are used as tensile reinforcement in concrete beams.

Evan C. et al. studied the shear strength of large concrete members with FRP reinforcements and analyzed the shear performance on 11 large concrete beams that are longitudinally reinforced with GFRP with or without stirrups considering the member flexural reinforcements ratio, member depth, and the amount of shear reinforcement as variables. Based on the obtained results, it can be concluded that concrete beams that are reinforced with FRP or normal steel show similar shear strength. The weak bending area of FRP was shown to be protected by multiple layers of longitudinal FRP bars. For concrete members with lower reinforcement ratio and higher longitudinal strains there seemed to be little effect of adding

stirrups. The significant impact and usage of stirrup can be efficient for the concrete beams with higher reinforcement ratio and lower longitudinal strains [24].

3.6 FLEXURAL BEHAVIOR OF REINFROCED CONCRETE BEAM REINFORCED WITH HYBRID REINFORCEMENT

Ilker Fatih et al. studied the flexural behavior of the concrete beams reinforced with a hybrid of steel and FRP (Fiber Reinforced Polymer) and developed a numerical method for estimating deflection, curvature, and moment capacity of the beams that have hybrid reinforcement. Forty- six (46) beams were casted and tested in the lab.

Based on the data achieved, the researchers concluded that the experimental results and predicted deflection of hybrid FRP and steel, moment capacity, and curvatures were all in good agreement. The study concluded that hybrid beams of FRP and steel increases the ductility and stiffness of the beams. FRP plays an important role to resist loads when yielding of steel occurs in over reinforced sections. Beams reinforced with steel and GFRP showed remarkable reduction for the initiation of the first crack and yielding of the steel reinforcement compared to the hybrid of CFRP and steel beams [25].

Michelle Theriault et.al. studied the effects of concrete strength and FRP ratio reinforcement on the flexural behavior of concrete beams and examined the crack width, crack spacing, load deflection, ultimate capacity and modes of failure of the concrete beams.

Twelve (12) concrete beams, each with similar dimensions of 130 x 180 x 1800 mm were reinforced with FRP rods.

Concrete beams were subjected to four-points flexural testing and were also instrumented with LVDTs to measure deflection. Strain gages were also used to monitor and measure the deformation as well as an automatic data acquisition system used to observe the loading, mid span deflection, and deformation of the concrete and reinforcements in the concrete beams. The study concluded that the cracks spacing has no correlation between the concrete strength and reinforcement ratio. However, residual crack width decreases as reinforcement ratio increases and residual crack is independent of the concrete strength. Ultimate moment capacity is directly proportional to the concrete strength and reinforcement ratio. The deflection occurred in the mid- span as the applied load increased and further cracking appeared in the beam as the applied moment exceeded the cracking moment which caused the stiffness to decrease [26].

H.Y. Leung et al. studied the flexural behavior of concrete beams reinforced with glass fiber reinforced polymer and steel rebar as a hybrid reinforcement system. Seven beams, each with the dimensions of 150 x 200 x 2500 mm were casted and tested under four points loading. Two different kinds of beam reinforcements were placed in two different level of tension zone and Table 3.5 shows more details of the specimens. Figure 3.5 shows the test setup of the tested concrete beams.

Table 3.5: Details of the casted specimen (27)

Beam designation	Designed concrete strength (MPa)	Number of steel rebars	Number of GFRP rods	Balanced reinforcement ratio (%)	Actual reinforcement ratio (%)	Beam classification
L0 (reference)	30	2	Nil	2.84[a]	0.81[b]	Under-reinforced
L1	30	Nil	2	0.45[a]	0.59[c]	Over-reinforced
L2	30	2	2	0.05[d]	0.59[c]	Over-reinforced
L5	30	2	3	0.05[d]	0.89[c]	Over-reinforced
H1	50	Nil	2	0.63[a]	0.59[c]	Under-reinforced
H2	50	2	2	0.23[d]	0.59[c]	Over-reinforced
H5	50	2	3	0.23[d]	0.89[c]	Over-reinforced

Notes: [a] use equation (1); [b] use equation (2); [c] use equation (3); [d] use equation (4)

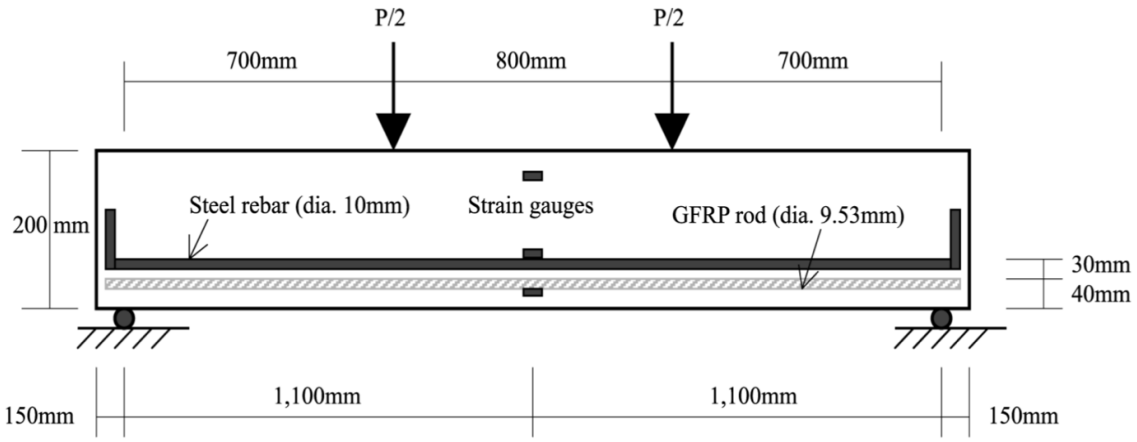

Figure 3.4: Experimental test setup details (27)

Four of the seven beams were casted with lower strength concrete while the remaining three were casted with High Strength Concrete beams. Each beam was tested in four-point bending. Minor cracks started appearing on the tension surface of the concrete when the load was applied and when the applied load was increased, the cracks became wider. Flexural cracks were developed in the bottom of the beams and during the first 35 kN both strains of concrete and steel were increased linearly. After that, the steel yield stayed constant and as the applied

load increased, the horizontal mid-span deflection plateau was found. Figure 3.6 shows the maximum loads and mode of failure of the beams.

Table 3.6: Details of beams maximum load and failure mode (27)

Beam	Maximum load (kN)	Failure mode
L0 (reference)	39.3	Steel yielding and compression concrete crushing
L1	34.2	GFRP slippage/bond failure
L2	63.5	Concrete crushing at one of the loading points
L5	65.9	Concrete crushing/concrete splitting at steel level
H1	36.4	GFRP slippage/minor rupture of GFRP rod
H2	60.3	Concrete crushing at one of the loading points
H5	77.3	Shear failure with minor concrete crushing

The authors conclude that flexural strength of concrete beams using hybrid reinforcement is higher relative to the concrete beams that have only reinforcement of either steel or GFRP. Increasing the strength of concrete caused the concrete beams to have larger flexural and shear capacities. Also, increasing the strength of the concrete increased the deflection capacity of the concrete beams during the failure [27].

CHAPTER 4: EXPERIMENTAL PROGRAM SETUP

4.1 INTRODUCTION

Fiber Reinforced Polymers or FRPs have been considered an excellent longitudinal replacement option for normal steel rebar to prevent corrosion and to extend concrete members service life. Concrete is a widely used common structural material that is being reinforced with normal steel bars to maintain the strength and integrity of the concrete members. Due to the metallic characteristic of steel reinforcement, concrete members are easily subjected to corrosion. The corrosion of steel in concrete beams is normally caused by harsh environments, especially in coastal, tropical, or desert locations where high chloride levels can accelerate the rate of decay. Normally exposed elements deteriorate first and the actual corroded reinforcement is not visible. It can take 5 to 15 years of active corrosion before the cracks start to initiate in the concrete members [29]. Every year, millions of dollars are spent fixing the corrosion problem in concrete structures.

4.2 EXPERIMENTAL PROGRAM

During this research, a total of 5 beams were designed and divided into four groups: the first group of beams is longitudinally reinforced with Carbon Fiber Reinforced Polymer (CFRP) grid without stirrups. The second group consists of beams reinforced by Glass Giber Reinforced Polymer (GFRP) grid without stirrups. The third group is reinforced with hybrid of CFRP grid with steel rebar and the fourth group of concrete beams is reinforced with hybrid of GFRP grid and steel. Reinforced concrete beams in the fourth group is the control beam that does not have stirrups. All beams were made form High Strength Concrete (HSC). Wooden forms were used for casting the concrete beams and they were casted in the structural

engineering laboratory. Wooden formworks were removed 24 hours after casting and then the specimens were covered with wet towels for 28 days of curing. The beams were 7 feet long, 12 inches thick, and 6 inches wide.

4.3 MATERIALS

4.3.1 FORMWORKS

Wooden Formwork is a temporary structure that contains poured fluid concrete to mold the concrete beam in the required dimensions and to hold the concrete beam in shape until the concrete is hardened. Each formwork was built to be 8 feet long, 13 inches thick, and 8 inches wide edge to edge. For the experiment, 5 wooden formworks were built and the inside faces of the forms were sprayed with grease to avoid water absorption during concrete casting. Reinforcements were placed inside the formwork and 0.5 inch high seats were attached to the reinforcement to establish 0.5 inch of concrete cover on the compression side and 1.0 inch on the bottom side (tension side). Figure 4.1 shows 5 wooden formworks used in this study.

Figure 4.1: Prepared wooden formwork for concrete beams

4.3.2 REINFORCEMENTS

Plain concrete is widely and mainly used for concrete structures due to its remarkable compressive strength. However, it is very weak in tension; thus, reinforcements are needed to resist tensile strength results from external loading. After the concrete sets and hardens, a new composite reinforced concrete section is formed. Reinforced concrete works very well in tension or/and compression [30]. In the experiment, five beams have three different kinds of reinforcements. CFRP, GFRP, and steel rebar were used as main reinforcements and were placed in the bottom of the formwork to work as tension reinforcements. Since the goal of this study is to examine the shear behavior HSC concrete beams, no stirrups or shear reinforcements were used. No. 5 rebar steel was used, where the first and last 5 inches of each rebar was bent to avoid slippage and provide better bonding between the rebar and concrete. The carbon fiber reinforced polymer and glass fiber reinforced polymer grids were also cut for length of 82 inches long and 5 inches wide. The first beam was reinforced with GFRP, the second beam was reinforced with CFRP, the third beam was reinforced with GFRP hybrid with steel, the fourth and fifth beams were reinforced with hybrid of CFRP and steel. The reinforcements were attached to the seats and then placed in the formwork. For hybrid beams, FRP was placed under two steel rebar and they were attached and tied to each other by a narrow metallic wire.

Table 4.1: Summary of the beam characteristics

Reinforcement Type	Length (in.)	Clear Span (ft.)	h (in.)	b (in.)	Bottom Reinforcement	a	Stirrups
CF_MN_2	84	6.16	12	6	CFRP grid	2	No
GF_MN_2	84	6.16	12	6	GFRP grid	2	No
CF_ST_MN_2.5	84	6.16	12	6	CFRP grid + 2#5 Steel bars	2.5	No
CF_ST_MN_2	84	6.16	12	6	CFRP grid + 2#5 Steel bars	2	No
GF_ST_MN_2	84	6.16	12	6	GFRP grid + 2#5 Steel bars	2	No

Figures 4.2 to 4.7 show the reinforcement types used in this study, while Figures 4.8 to 4.12 show all the beams formwork with all reinforcement bars/grids installed.

Figure 4.2: GFRP grid

Figure 4.3: #5 steel rebar

Figure 4.4: Carbon FRP

Figure 4.5: CFRP hybrid with #5 steel bar

Figure 4.6: CFRP grid with seat

Figure 4.7: GFRP hybrid with steel

Figure 4.8: *CFRP hybrid with steel*

Figure 4.9: CFRP Hybrid with steel

Figure 4.10: Beam Three – CFRP-only

Figure 4.11: Beam Four – GFRP-only

Figure 4.12: Beam Five - CFRP hybrid with steel

4.3.3 HIGH STRENGTH CONCRETE (HSC)

The High Strength Concrete was prepared by a combination of fly ash, Portland cement, high range water reducer, water, fine silica sand, and steel or organic fiber. The ductile behavior of these materials is a first for concrete with the capacity to deform and support flexural and tensile load even after the initial crack appears in the concrete structure [31]. During the experiment, HSC with strength of 9,000 Psi (pounds per square inch) was prepared and delivered by Central Pre-Mix Concrete Cooperation, Pullman, Washington. The concrete truck was parked outside the laboratory, transported by wheelbarrow, and then shoveled into the wooden formwork that had the reinforcements. A concrete vibrator was used to help the concrete mix move easily in the formwork. After the formworks were filled with concrete, the

top surface of the concrete was finished and leveled using a metal finishing trowel. Finally, clamps were attached to the formwork to avoid any kind of buckling and to further support the shape of the beam until the concrete hardens as shown in Figures 4.14 to 4.17.

Material	Batched Quantity	Moisture (%)	Actual Water (gl.)
3/4" CUBED	3020 lb.	0.10% M	-
BLEND SAND	2640 lb.	4.07% A	12 gl.
TYPE I-II	1490.0 lb.	-	-
DARAVAIR (AIR ENTRAIN.)	5.00 Oz	-	-
DARACEH (Con. SUPERPLASTICISER)	57.00 Oz	-	-
WATER	45.0 gl.	-	-
WATER/CEMENT RATIO	0.323	-	-

Figure 4.13: Properties of High Strength Concrete

Figure 4.14: Premix concrete truck

Figure 4.15: Pouring concrete into formwork

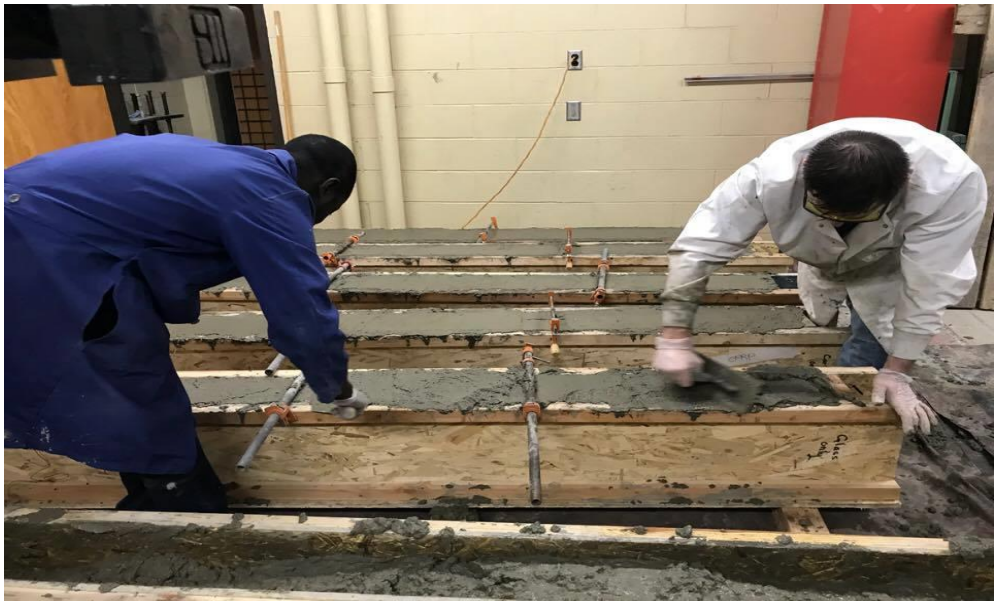

Figure 4.16: Leveling surface of concrete

Figure 4.17: Casted concrete beams with clamps

4.3.4 STRAIN GAGE

Strain gage is used to measure strain and convert weight, force, tension, etc., into electrical resistance. It calculates the deformation and displacements that occurs when an external load is applied to a stationary object. In the experiments, two strain gages were attached to each reinforcement bar in order to capture strain when load was applied. To install the strain gages on the surface of the reinforcing bars, various steps have been accomplished. First, the locations of strain gages were marked at 31 inches away from the midpoint of the reinforcements. Secondly, an electric grinder was used to grind the marked surface and was cleaned with baking soda water. After drying the cleaned area, a super glue instant-set epoxy was placed using a syringe to attach the strain gages to the reinforcement's surface. The glue dried for 10 minutes, then electrical tape was applied under the exposed lead wires. Electrical

tape was then wrapped around the entire strain gage area while also adding a thin layer of epoxy to improve the mechanical protection of the strain gages during concrete casting. Figures 35 to 38 show the steps performed to install strain gages.

Figure 4.18: Strain gage attached to rebar with glue

Figure 4.19: Strain gage with attached tape

Figure 4.20: Strain gage with tape under lead wire

Figure 4.21: Strain gage with complete attachment

4.3.5 DATA ACQUISITION SYSTEM

Data acquisition system was used to collect the strain from the specimen when exposed to applied load. LVDT also known as Linear Variable Differential Transformer is an electromechanical transmitter that measures linear displacements and converts the rectilinear motions of an object to which it is coupled mechanically into a corresponding electrical signal [32]. During the experimental testing, LVDT was positioned at all beams mid span. LVDT was connected to the Data Acquisition system to monitor the deflection-time history. The Data Acquisition system used in this project is Expert Data Logger which processes 46 analog input channels at both low and high rates of sampling. This measurement data can be accurately acquired, dependently stored, and transmitted to the PC for further evaluation [33]. The strain gages and LVDT were connected to via plug-in crew terminals and the data logger was being configured from a PC as shown in Figure 4.22-24.

Figure 4.22: Strain gage attached to Expert Data Logger

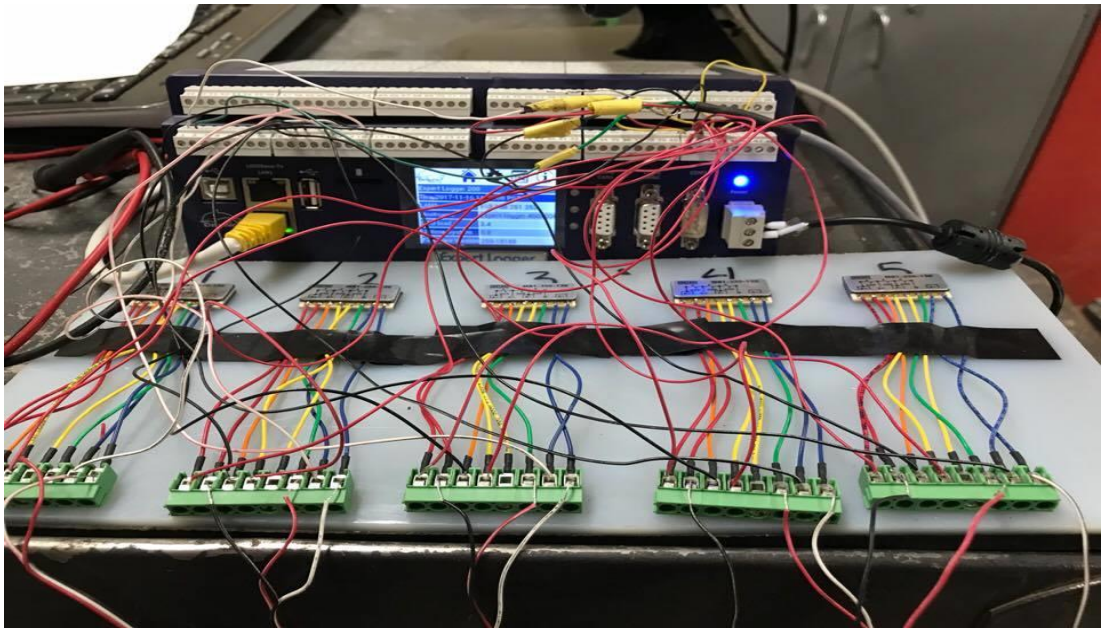

Figure 4.23: Expert Data Logger connection to strain gages and LVDT

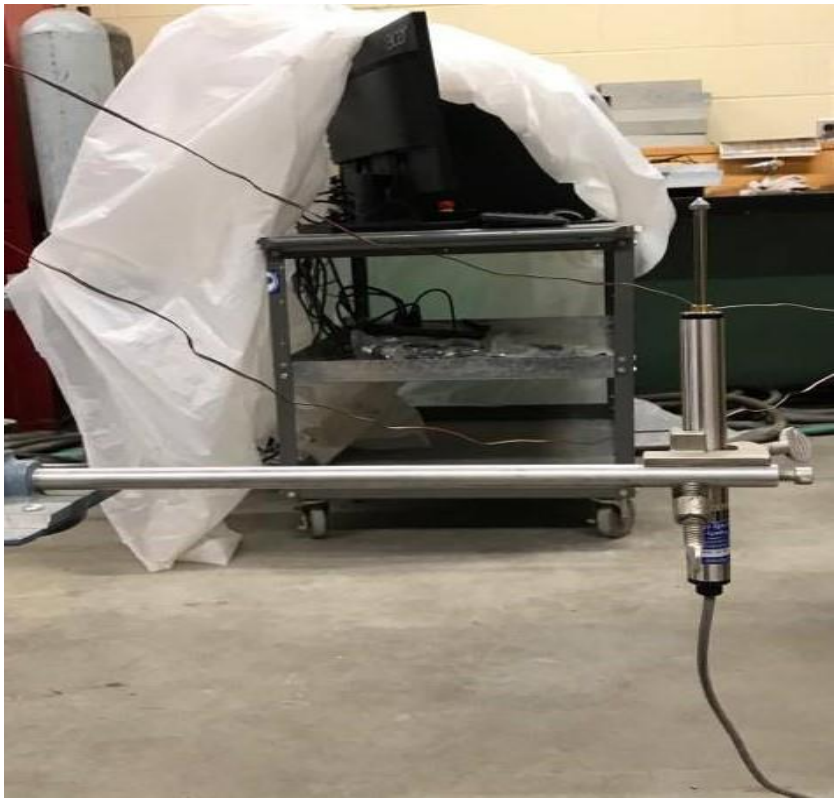

Figure 4.24: LVDT attached to Expert Data Logger under specimen

4.4 TEST SETUP

Five reinforced HSC beams were tested under four-point loading and the load was generated by servo-valve hydraulic single ended fatigue-rated actuator. The load was transformed to a spreader beam which was bolted to the actuator [34] as shown In Figures 42 and 43. The spreader beam was supported by two steel adjustable rollers. The concrete specimens were also supported by two rollers and the monotonic load was applied to all beams under displacement control at a rate of 1 mm/min. The beams were 36 inches above the ground, and the LVDT was placed under the beam at the midspan.

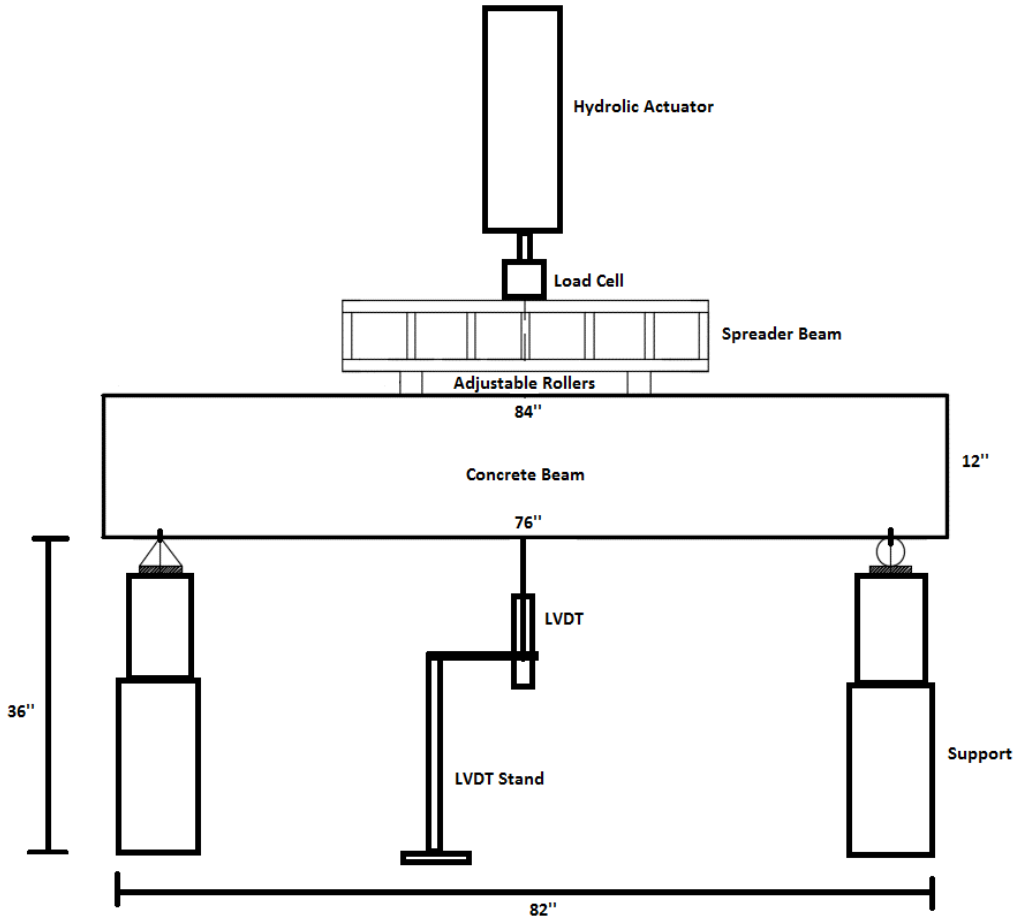

Figure 4.25: Geometry of experimental test setup

Figure 4.26: Experimental test setup of the concrete beams

4.5 BEAM NAMING

To name the beams, I used the procedure below:

1. CF_MN_2: Concrete beam with tensile reinforcement of CFRP grid, with shear span of 2 and no stirrups
2. GF_MN_2: Concrete beam with tensile reinforcement of GFRP grid with shear span of 2 and no stirrups
3. CF_ST_MN_2.5: Hybrid concrete beam with tensile reinforcement of CFRP grid and 2#5 steel rebar, shear span-to-depth ratio of 2.5 and no stirrups

4. CF_ST_MN_2: Hybrid concrete beam with tensile reinforcement of CFRP grid with 2#5 steel rebar, shear span-to-depth ratio of 2, and no stirrups
5. GF_ST_MN_2: Hybrid concrete beam with tensile reinforcement of GFRP grid with 2#5 steel rebar, shear span-to-depth ratio of 2, and no stirrups

Where:

ST = Steel

GF = GFRP

CF = CFRP

MN = Monotonic load

2 = Shear span-to-depth ratio of 2

2. 5 = Shear span-to-depth ratio of 2. 5

CHAPTER 5: RESULTS AND DISCUSSIONS

This chapter presents the experimental results of testing five HSC beams under monotonic load. All beams were reinforced by steel and fiber composites to act as a hybrid reinforcement without web reinforcements. The main goal of testing all the beams is to investigate the effect of such reinforcement on the shear behavior and beams capacity. The results present the load-displacement history, load-strain history, and mode of failure. The results were compared to the Canadian Educational Module Code to see the applicability of its design equations in predicting the moment and flexural capacity of HSC beams reinforced with hybrid reinforcements.

5.1 LOAD-DEFLECTION RESPONSE

The load-deflection history presents the deformation of five reinforced concrete beams tested under applied monotonic load. The load-deflection response of the five reinforced concrete beams with the ultimate loads versus the maximum deflections are shown in Figure 5.1.

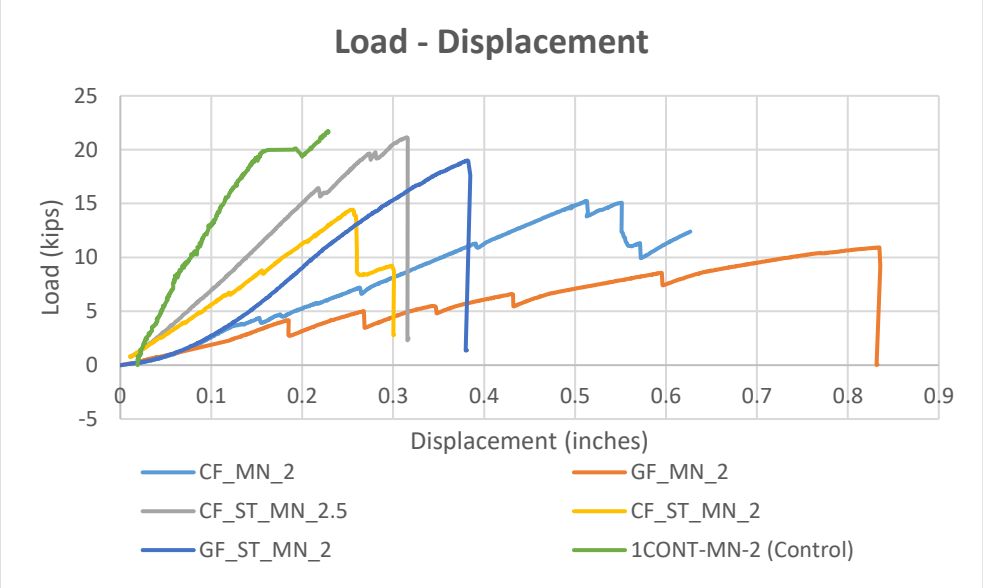

Figure 5.1: Load and deflection curve of the reinforced concrete beams

Five identical specimens were casted with no shear reinforcement and tested with shear spans of 2.0 and 2.5. The load-displacement of the beams were recorded. Both the deflection and the applied load were increased until the beams failure. Beam GF_MN_2 did not reach the ultimate capacity due to testing malfunction, however the other beams reached their ultimate load capacities. The control beam that was only reinforced with two #5 steel bars had the highest ultimate load capacity of 21.7 kips with the lowest deflection 0.29 inches. Beam CF_MN_2 failed in shear when the ultimate load capacity of 15.08 kips was reached with the deflection of 0.63 inches. GF_MN_2 did not reach its ultimate load capacity and failed in shear with maximum load of 11.05 kips and a corresponding displacement of 0.84 inches. On the other hand, the hybrid beams did perform well and had lower deflection relative to beams reinforced with pure FRP. Beam CF_ST_MN_2.5 with shear span of 2.5 had the maximum load capacity of 21.1 kips with deflection of 0.32 inches. Beam CF_ST_MN_2 reached the maximum load capacity of 14.4 kips with deflection of 0.30 inches, and that is attributed to a slippage failure that happened during testing and made the load-carrying capacity decrease compared to beam CF-MN-2.5. Finally, beam GF_ST_MN_2 reached the maximum load capacity of 19.1 kips with deflection of 0.38. Comparing the obtained results with the control beam, beam CF_ST_MN_2.5 with shear span of 2.5 showed similar load capacity and deflection. Beam GF_MN_2 did not reach its ultimate load capacity, indicating 50.82% less load capacity with the maximum mid span deflection of 120.93% relative to control beam. It is important to note that beam GF_MN_2 had the poorest performance compared to the rest of the beams due the low stiffness of GF compared to CF.

Table 5.1 shows the maximum load capacity, maximum experimental deflection, and the percentage of maximum applied loads relative to the control beam (1CONT_MN_2)

reinforced with two #5 steel bars and with no shear reinforcement. Concrete beams reinforced with a hybrid of FRP grid in addition to steel bars demonstrated different responses to the maximum applied load. The highest load was obtained from the hybrid beam CF_ST_MN_2.5, and the lowest was corresponding to beam GF-MN-2, which is attributed to the lower elastic modulus that GF grids have.

Table 5.1: Maximum - deflection for 5 specimens

Beam Type	P max (lb.) Maximum Load	Exp. Maximum Deflection (in)	% Load Differences
Control Beam (ICONT-MN-2)	21740.1	0.299	100
CF_MN_2	15086.1	0.63	69.3933
GF_MN_2	11050	0.84	50.828
CF_ST_MN_2.5	21153.2	0.32	97.3008
CF_ST_MN_2	14426.8	0.30	66.3606
GF_ST_MN_2	19153.5	0.38	88.1026

To further study the load-deflection behavior, the energy absorption was calculated by considering the area under the load–displacement curve. Energy Absorption Capacity is an important property that shows beams toughness and ductility. The reinforcements used in the concrete beams is motivated and supported by their energy absorption capacity. To find the energy absorption capacity of the all beams, the area under each load–displacement curve was calculated. Since the values for load–deflections are already determined using equation (1), the energy absorption capacity of each beam has been found. The beam reinforced with glass fiber only experienced the highest toughness (277%), higher than the control beam, while the

lowest toughness was accompanied by the failure of the beam reinforced with CFRP-only (66%) lower than the control beam.

$$Energy\ Absorption\ Capacity = \sum \frac{\Delta deflection\ \Delta load}{2} \quad (1)$$

Thus, Table 5.2 shows the energy absorption capacity of the concrete beams.

Table 5.2: Energy absorption capacity of the concrete beams

Energy Absorbed in Kips*Inches			
Reinforcement	**Beams Name**	**Area under the Curve (in.^2)**	**%Area under the Curve**
Steel-only (control)	ICONT-MN2	1.78	100.0
Carbon Fiber (CFRP)	CF_MN_2	1.18	66.3
Glass Fiber (GFRP)	GF_MN_2	4.93	277.0
Hybrid (CFRP + 2#5 Steel)	CF_ST_MN_2.5	3.15	177.0
Hybrid (CFRP + 2#5 Steel)	CF_ST_MN_2	1.83	102.8
Hybrid (GFRP + 2#5 Steel)	GF_ST_MN_2	3.04	170.8

The results indicate that the beam GF_MN_2 had the highest energy absorption of 177% while beam CF_ST_MN_2 had the lowest energy absorption of -33.7% relative to the control beam.

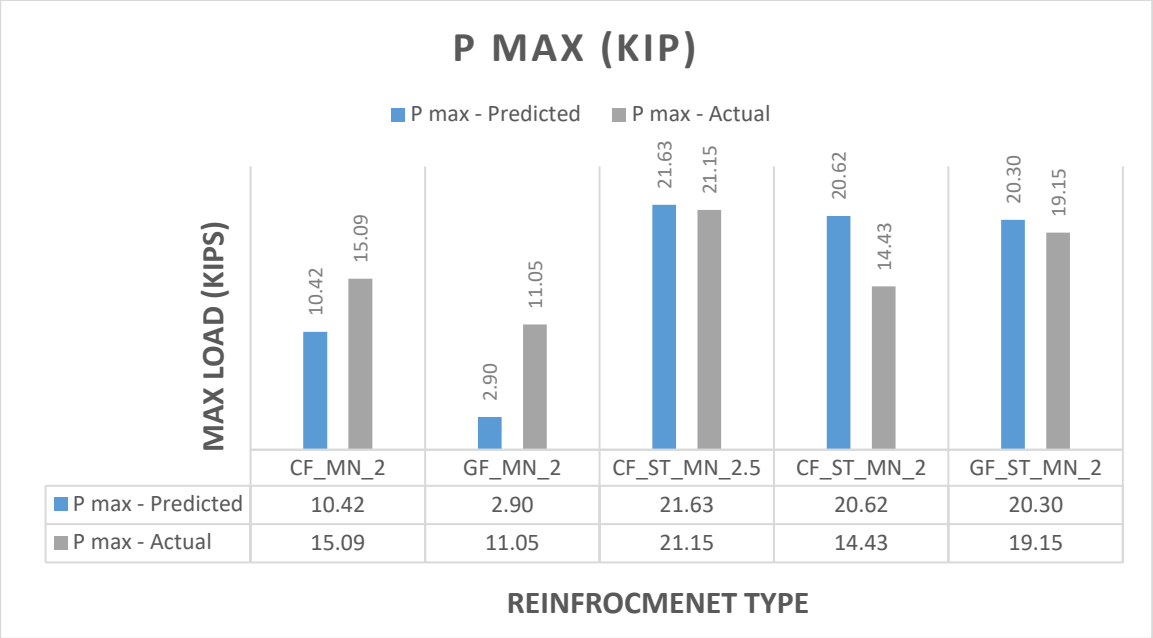

Figure 5.2: Actual and experimental maximum load on RC beams

Figure 5.2 shows that beam GF_MN_2 has the lowest maximum load capacity of 11.06 kips experimental and 2.90 kips analytical and beam CF_ST_MN_2.5 has the highest load capacity.

5.2 LOAD –STRAIN HISTORY

Strain in a concrete beam is the response of the beam to an applied stress. When stress is applied, the beam deforms and as a result the material also deforms. To better understand the strain of a beam reinforced with FRP-only and with hybrid reinforcement, the strain behavior of concrete beams under monotonic four-point load will be discussed. Strain gages were attached to the tensile reinforcements of all the beams to collect the strain for each beam when load was applied. All beams failed in shear as expected (no web reinforcement) and the failure was sudden once the ultimate shear strength was reached. Figures 5.3 to 5.7 show the load-strain history.

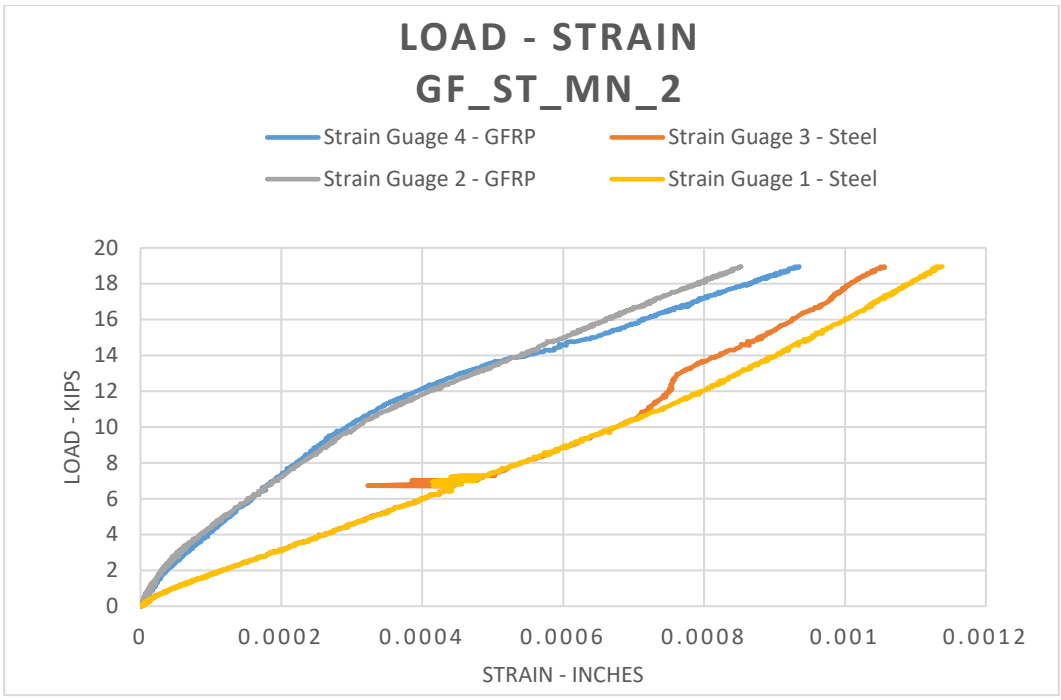

Figure 5.3: Load - strain history curve of hybrid - GFRP and steel

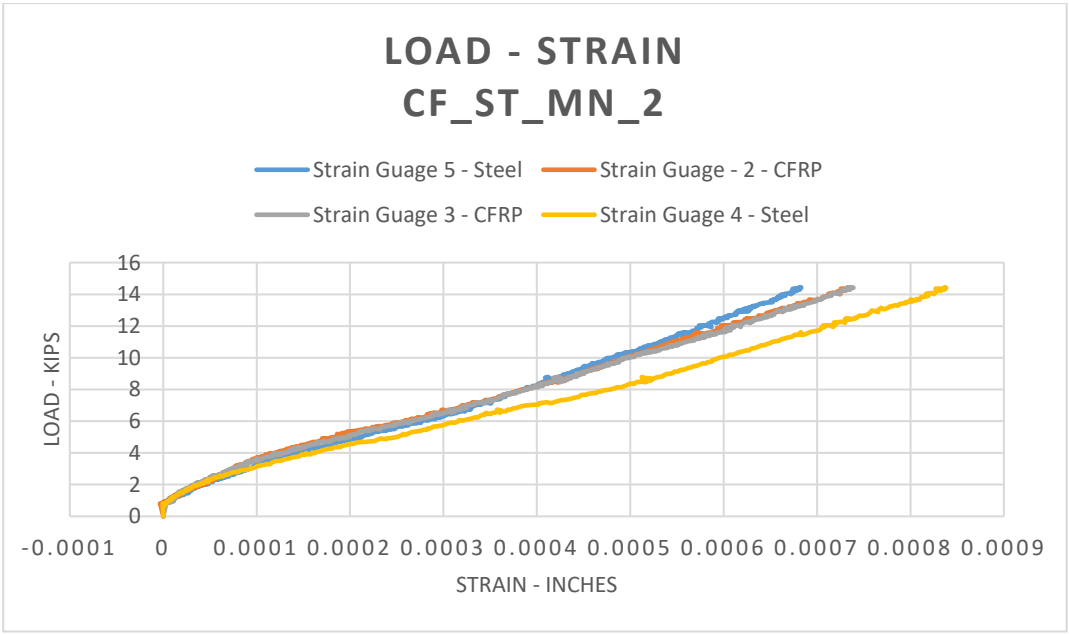

Figure 5.4: Load – strain history curve of hybrid - CFRP and steel

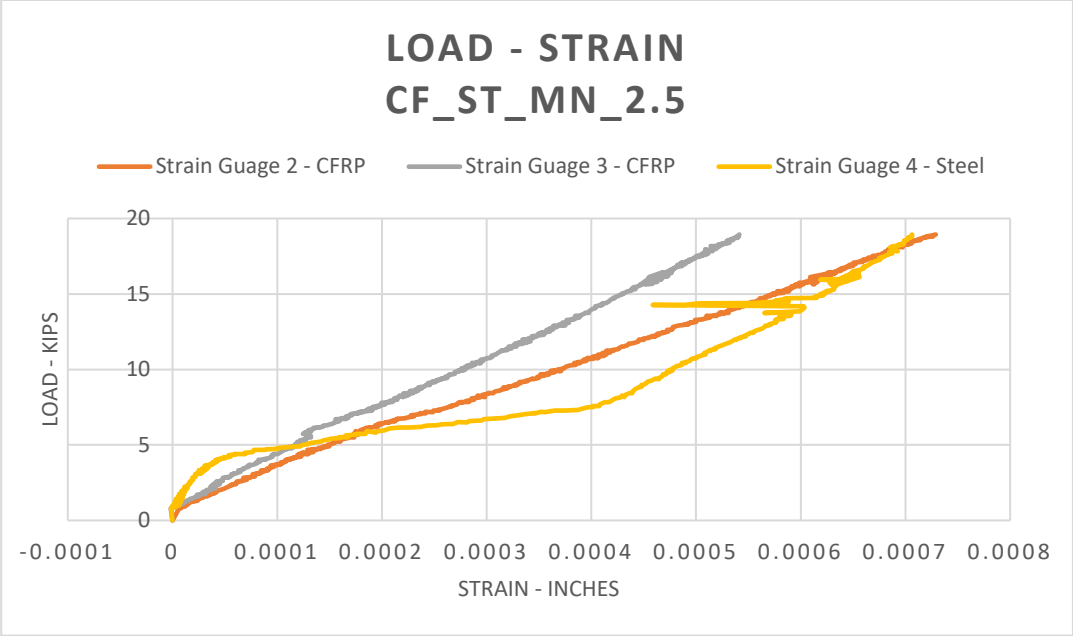

Figure 5.5: Load – strain history curve of hybrid - CFRP and steel

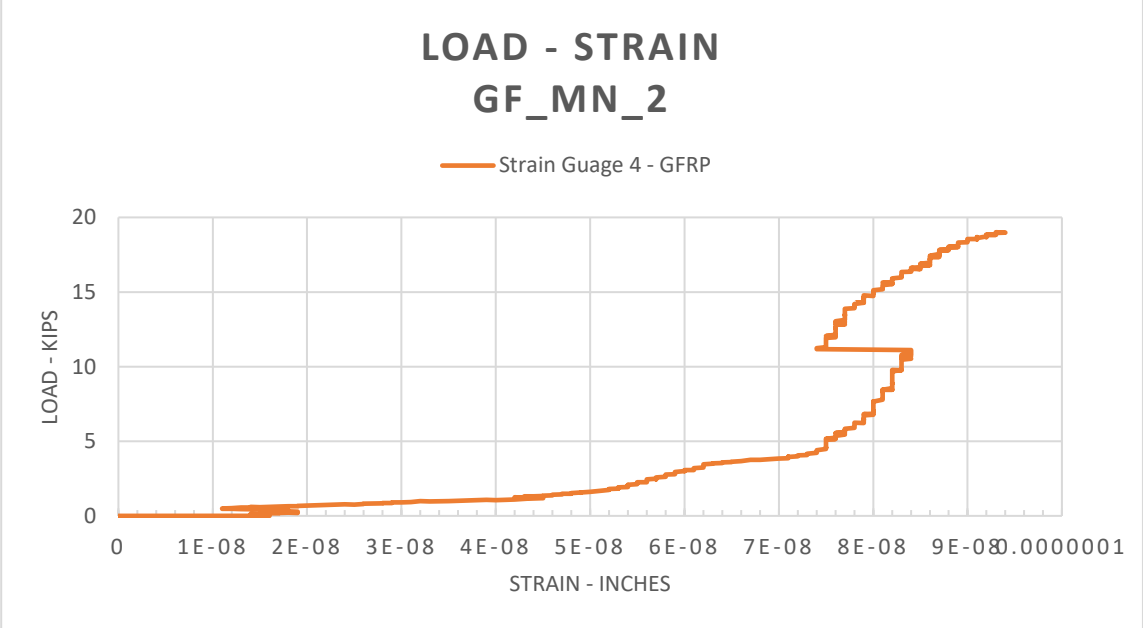

Figure 5.6: Load – strain history curve of GFRP

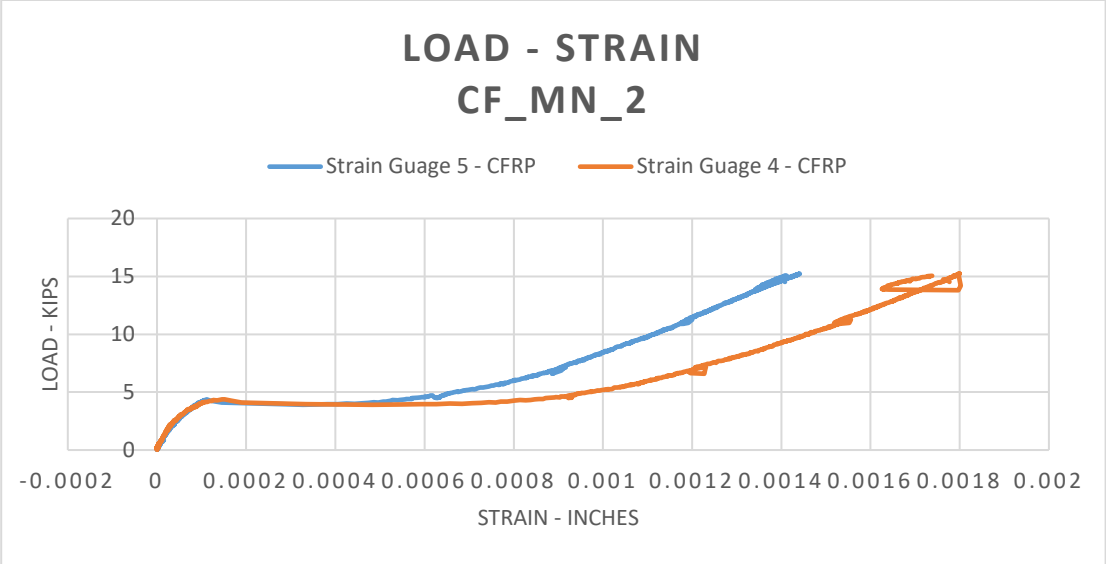

Figure 5.7: Load - strain history curve of CFRP

The load-strain relationship was captured during the testing. Maximum of 2 strain gages for FRP-only and 4 strain gages for hybrid reinforced beams were attached at the midspan of the main bottom reinforcements to capture the behavior under the monotonic load. As the load increased, tension strain in the bottom reinforcements increased until the sudden failure of the beam occurred. The bottom tensile strain of all beams did not reach the yield strain (2069 micro strain) and due to the failure of concrete before steel yielding, the concrete beams failed. All beams failed suddenly due to inclined major shear cracks extended from the left or right support to the location where the point load was applied. The strain response of beam CF_MN_2 as in Figure 5.7 was increasing rapidly until 4.2 kips and then strain increased slowly as the load increased until the ultimate load of 15.08 kips was reached. At that time, the CFRP did not reach the ultimate rupture strain of 14000 micro strain. For beam GF_MN_2 in Figure 5.6, the strain response of the main reinforcement was increasing slowly with an increasing applied load until the beam failed in shear at 11.05 kips, but it did not

reach its ultimate load capacity. In Figure 5.5, the strain-load history of hybrid beam under a shear span-to-depth ratio of 2.5 did not reach its yield strain as well and the beam failed in shear at its ultimate load capacity of 21.1 kips which is the highest load capacity among all the tested beams. Figure 5.4 shows that the strain increased steadily as the applied load increased and the beam failed in shear at the ultimate load capacity of 14.4 kips. Finally, Figure 5.3 shows that the strain response of the main reinforcement increased as the load increased until the beam failed in shear at 19.1 kips. The beams main reinforcement strain did not exceed the yield strain due to the formation of large cracks on the sides that lead to sudden shear failure.

The load-strain history of all the beams show that beam reinforced with CFRP grid has a higher strain but lower load capacity compared to GFRP grid. In contrast, the CFRP grid has lower strain but higher load capacity relative to GFRP grid. Hybrid beams with GFRP grid have both higher strain and load capacity compared to the hybrid CFRP grid. The average strain of CFRP grid under a shear span-to-depth ratio of 2.5 was lower than the load-strain history of CFRP and GFRP grid in other hybrid beams. Since the steel has a high modulus of elasticity, the strain performance of the steel under applied load was higher compared to CFRP and GFRP grid. Overall, the GFRP-only had the lowest failure strain and the highest load capacity.

5.3 MOMENT CAPACITY

Moment capacity is the ability of an applied force that causes a twisting or turning effect about an axis to a concrete beam. To find the ultimate moment, the Canadian Educational Module Code (29) code of fiber reinforcement provides an equation (2) to estimate the

moment capacity of beams reinforced with FRP, while ACI 318-16 equation (3) predicts moment capacity of conventional beam reinforced with conventional steel bars.

$$M_{u\,(frp)} = \emptyset_{frp} A_{frp} f_{frpu} (d - \frac{\beta c}{2}) \quad (2)$$

$$M_{u\,(steel)} = \emptyset_{steel} A_{steel}\, f_{steelu} (d - \frac{\beta c}{2}) \quad (3)$$

Where:

a = Shear span-to-depth ratio of reinforced concrete beam

$M_{u\,(frp)}$ = Ultimate moment of FRP reinforcement

$M_{u\,(steel)}$ = Ultimate moment of steel reinforcement

$\emptyset_{frp}$ = Material resistance factor of FRP reinforcement

f_{frpu} = Ultimate tensile strength of FRP reinforcement

f_{steelu} = Ultimate tensile strength of grade 60 steel reinforcement

β = Stress – block parameter for concrete at a strain less than ultimate

c = Depth of neutral axis

To estimate the ultimate moment of hybrid (steel + FRP) reinforced concrete beams, equation (4) was used. Tables 5.4 and 5.5 show the details of the strength reduction factors and the mechanical properties that were used in the calculations.

$$M_u = M_{u\,(frp)} + M_{u\,(steel)} \quad (4)$$

Table 5.3: Characteristic of the concrete beams

Reinforcement Type	**Shear Span (a)**	**λ** (Lambda)	**f'_c (psi)**	**b (in.)**	**d (in.)**	**α**	**β**
CF_MN_2	22	1	9000.0	6	11	0.7	0.85
GF_MN_2	22	1	9000.0	6	11	0.7	0.85
CF_ST_MN_2.5	27.5	1	9000.0	6	11	0.7	0.85
CF_ST_MN_2	22	1	9000.0	6	11	0.7	0.85
GF_ST_MN_2	22	1	9000.0	6	11	0.7	0.85

Table 5.4: Material Resistance Factor

Material Resistance factor		
Material	**Notation**	**Factor**
Concrete	Øc	0.75
Steel	Øs	0.90
CFRP	Øfrp	0.80
GFRP	Øfrp	0.55

Table 5.5: Tensile strength, elastic modulus, and compressive strength

Reinforcement Type	**Tensile Strength $f_{frpu\ or\ steel}$ (Psi)**	**Elastic Modulus E_{frpu}(Psi)**	**Compressive strength (Psi)**
CFRP Grid	174045.3	14503.77	-
GFRP Grid	87022.6	43511.32	-
Concrete	-	-	10000
Grade 60 Steel	60000	29000.000	-

First, it needs to be determined if the section of the reinforced concrete beam will fail by tension failure or compression failure. When balanced failure reinforcement ratio is greater than reinforcement ratio, the section fails in tension. Otherwise, the beam will fail in compression.

Canadian educational module Code:

$$\rho_{balance\ (frp)} = \frac{f_{frpu}}{E_{frpu}} \tag{5}$$

$$\rho_{balance\ (steel)} = \left(\frac{0.85\beta f'_c}{f_y}\right)\left(\frac{87000}{87000 + f_y}\right) \tag{6}$$

Note: Balanced failure reinforcement ratio of steel and FRP were added to find the balanced failure reinforcement ratio of hybrid beams

ρ_w Is calculated using Canadian Educational Module Code equation (7):

$$\rho = \frac{A_{steel\ \&\ frp}}{b_w d} \tag{7}$$

Where:

$\rho_{balance\ (frp)}$ = Balanced failure reinforcement ratio

ρ_w = Reinforcement ratio

f_y = Steel tensile strength

E_{frpu} = Elastic modulas of FRP

f'_c = Concrete strength

b_w = Width of the concrete beam

d = Effective depth of the concrete section

Table 5.6 shows that all the reinforced concrete beams are predicted to fail in tension.

Table 5.6: Reinforcement ratio and balanced failure reinforcement ratio

Reinforcement Type	**ρ Reinforcement Ratio**	**ρ_b (balanced)**	
CF_MN_2	0.0023	0.0043	**> ρ frp: Breaks in Tension**
GF_MN_2	0.0019	0.0839	**> ρ frp: Breaks in Tension**
CF_ST_MN_2.5	0.0117	0.0684	**> ρ frp: Breaks in Tension**
CF_ST_MN_2	0.0117	0.0684	**> ρ frp: Breaks in Tension**
GF_ST_MN_2	0.0112	0.1481	**> ρ frp: Breaks in Tension**
Steel Grade 60	0.0094	0.0641	

To calculate the area of hybrid beams reinforcements, first the area of steel needs to be located, then the area of FRP reinforcement. Adding the area of FRP and steel will result in the area of hybrid beams reinforcement shown in the Table 5.7. The Canadian Educational

Module Code for FRP is used to estimate the area of CFRP and GFRP [36]. The area of the reinforcements are shown in the Table 5.7

Table 5.7: Area of the reinforcements

Reinforcement Type	$A_{frp\ or\ steel}$ (in.^2)
CF_MN_2	0.16
GF_MN_2	0.13
CF_ST_MN_2.5	0.78
CF_ST_MN_2	0.78
GF_ST_MN_2	0.75

The tensile stress resultant can be calculated directly using Canadian Educational Module Code equation (8):

$$T = \emptyset_{frp\ or\ steel} A_{frp\ or\ steel} f_{frpu\ or\ steelu} \quad (8)$$

Table 5.8: Tensile stress resultant of reinforced concrete beams

Reinforcement Type	T (Kips)
CF_MN_2	21581.6172
GF_MN_2	5860.754554
CF_ST_MN_2.5	58781.6172
CF_ST_MN_2	58781.6172
GF_ST_MN_2	44860.75455

The compressive stress resultant could be obtained using the following Canadian Educational Module Code equation (9):

$$C = \alpha \emptyset_c f'_c \beta b \quad (9)$$

Table 5.9: Compressive stress resultant of reinforced concrete beams

Reinforcement Type	C (Kips)
CF_MN_2	24097.5
GF_MN_2	24097.5
CF_ST_MN_2.5	24097.5
CF_ST_MN_2	24097.5
GF_ST_MN_2	24097.5

To calculate the depth of neutral axis (c) simply divide tensile stress over compressive stress, using Canadian Educational Module Code equation (10).

$$c = \frac{T}{C} \quad (10)$$

Table 5.10: Depth of neutral axis

Reinforcement Type	Calculated c (in.)
CF_MN_2	0.895595692
GF_MN_2	0.243210066
CF_ST_MN_2.5	2.439324295
CF_ST_MN_2	2.439324295
GF_ST_MN_2	1.861635213

Plugging the calculated values into the moment capacity equations, experimental moment capacity is shown in Table 5.11:

Table 5.11: Experimental moment capacity of reinforced concrete beams

Reinforcement Type	Moment Capacity (Kip ft.) Analytical
CF_MN_2	19.09860148
GF_MN_2	5.321875619
CF_ST_MN_2.5	49.56103493
CF_ST_MN_2	37.8019146
GF_ST_MN_2	37.21034424

Based on the experimental applied maximum load, actual moment capacity can be calculated, using Canadian Educational Module Code equation (11):

$$M_{u\,(actual)} = P_{max}a \qquad (11)$$

Table 5.12: Experimental moment capacity of reinforced concrete beams

Reinforcement Type	Mu (Kip ft.) Experimental Moment Capacity
CF_MN_2	27.66
GF_MN_2	20.26
CF_ST_MN_2.5	48.48
CF_ST_MN_2	26.45
GF_ST_MN_2	35.11

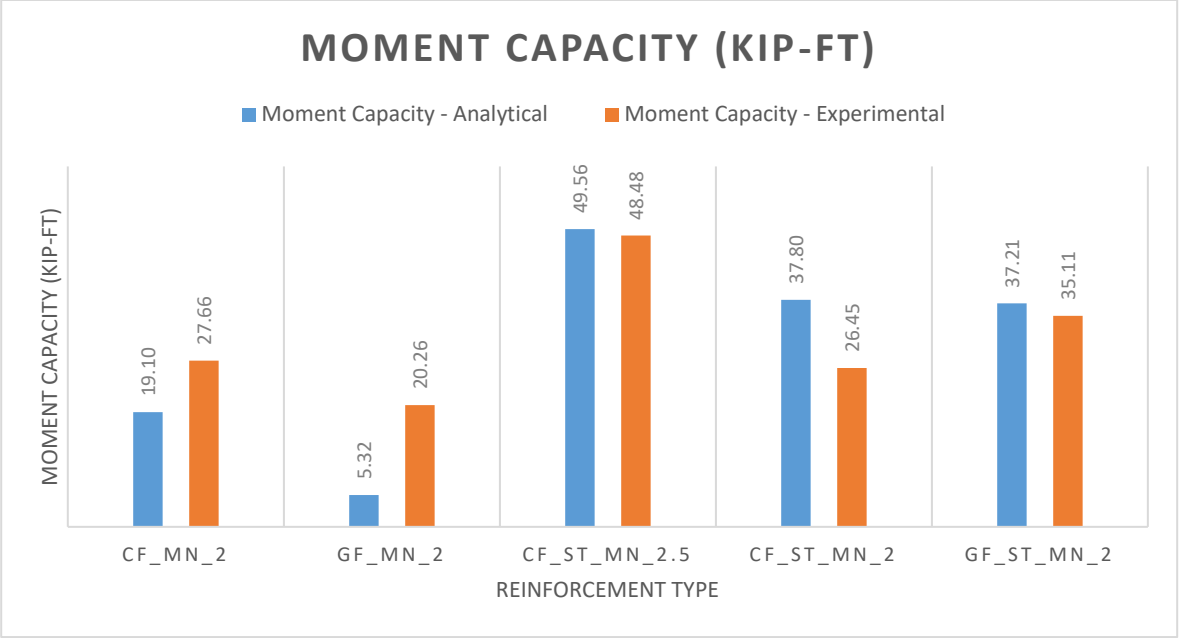

Figure 5.8: The bar chart shows the actual and experimental values of moment capacity

Figure 5.8 shows the actual and experimental moment capacities of the reinforced concrete beams. The experimental moment capacity is calculated based on the static load applied to each specimen while the analytical moment capacity is calculated using moment capacity equations provided by the Canadian code. Based on the results obtained in Figure 5.8, the values of experimental and analytical moment strengths are not in a good agreement and that is based on the reinforcement type. For beams reinforced with FRP-only, Equation (2) could be used to find a closer moment capacity prediction for the CFRP grid. However, Equation (1) was developed mainly for FRP bars, not grids. For hybrid beam reinforcement, Equations (2) and (3) were used to predict the moment capacity for beams with hybrid reinforcement for various shear-span-to depth ratios.

Figure 5.8 shows that beams reinforced with CFRP-only had discrepancies in moment capacity between predicted (19.10 kip-ft.) and experimental (27.66 kip-ft.). The beam reinforced with GFRP-only had a high percentage of difference between the experimental and

the analytical values (5.32 kip-ft. predicted versus 20.26 kip-ft. experimental). For the hybrid concrete beams with CFRP grid and steel, under the shear-span-to-depth ratio of 2 had the highest moment capacity (49.56 kip-ft. predicted and 48.48 kip-ft. experimental). The rest of the specimens that are reinforced with the hybrid of CFRP grid and steel (37.80 kip-ft. experimental and 26.45 kip-ft. experimental) and hybrid of GFRP grid and steel (37.21 kip-ft. experimental and 35.11 kip-ft. experimental) have a similar moment capacity.

5.4 SHEAR STRENGTH

Shear strength is the materials ability to resist forces that can cause the internal structure of the material to slide against itself. In different wording, shear strength is the strength of materials or components against the type of yield or structural failure where their materials or components fail in shear [35] as shown in the figure 5.9.

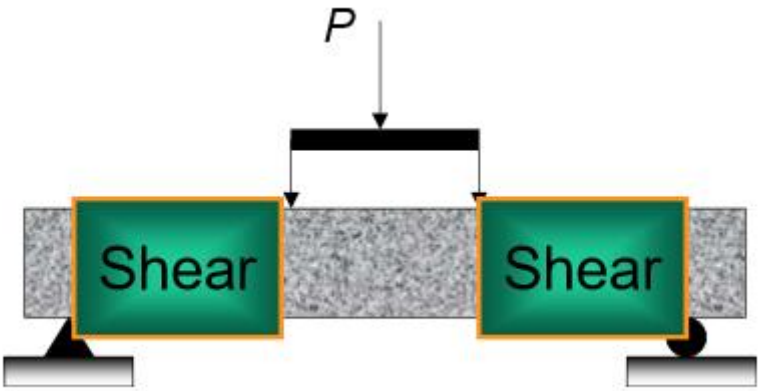

Figure 5.9: Location of shear force span

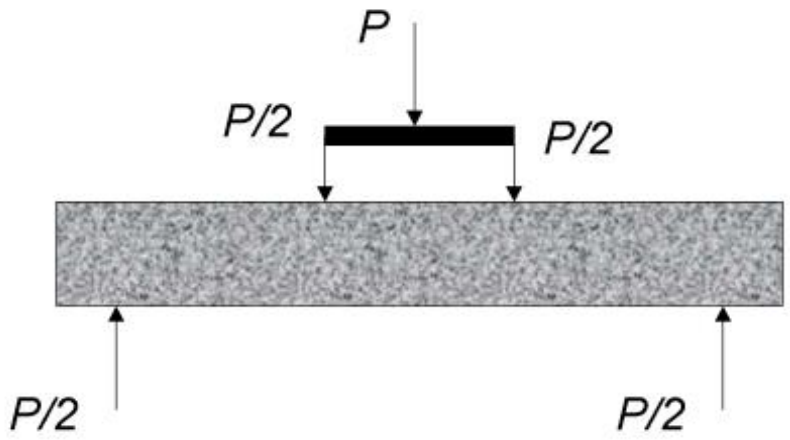

Figure 5.10: Geometry of shear force span

The shear strength is the sum of the shear strength provided by the effective concrete section and stirrups using Canadian Educational Module Code Equation (12):

$$V = V_c + V_s \quad (12)$$

Where:

V_c = the shear strength provided by the concrete

V_s = the shear strength provided by the stirrups

Since all the concrete specimens casted in the experiment do not have any stirrups or shear reinforcements, the shear strength is assumed to be resisted by the concrete web.

$$V_s = 0 \quad (13)$$

$$V = V_c + 0 \quad (14)$$

$$V = V_c \quad (15)$$

Using the ACI equations (16) and Equation (17), the experimental and actual shear strength of the reinforced concrete beams were experimental as following:

$$V_c = 2(\sqrt{f'c})b_w d \quad (16)$$

$$V_c = [1.9\lambda(\sqrt{f'c}) + 2500\ \rho_w \frac{V_u d}{M_u}]b_w d \quad (17)$$

Where:

$f'c$ = the compressive strength of the concrete

b_w = the width of the web

d = the effective depth of the section

ρ_w = longitudinal reinforcement ratio

V_u = shear force

M_u= the ultimate moment

λ = lightweight concrete modification factor

P max is the maximum applied load by the actuator that caused the reinforced concrete beam to fail in shear.

To calculate V_u, experimental $P_{Max\ (predicted)}$ needs to be determined and using the Canadian Educational Module Code Equation (18), value of P_{Max} can be obtained using Equation (18). Table 5.13 shows the shear force values obtained from the experimental testing,

$$P_{Max\ (predicted)} = \frac{Mu}{a} \quad (18)$$

Where:

$P_{Max\ (predicted)}$ = experimental applied load

Table 5.13: Experimental maximum load

Reinforcement Type	P max-Experimental (kip)
CF_MN_2	10.42
GF_MN_2	2.90
CF_ST_MN_2.5	21.63
CF_ST_MN_2	20.62
GF_ST_MN_2	20.30

After plugging in the obtained required values into equation 5 and 6, the experimental and actual shear strength can be obtained. To calculate the experimental and actual shear force, simply divide the $P_{Max\ (actual)}$ using ACI Equation (19) and (20):

$$v_{c\ (actual)} = \frac{P_{Max\ (actual)}}{2} \quad (19)$$

$$v_{c\ (predicted)} = \frac{P_{Max\ (predicted)}}{2} \quad (20$$

Table 5.14: Experimental and actual shear strength and shear force using two equations

Reinforcement Type	Vu (lb.) Experimental Equation (19)	Shear Strength (lb.) For Equation (16) - Analytical	Shear Strength (lb.) Equation (17) - Analytical	Vu (lb.) – Analytical Equation (20)
CF_MN_2	7543.05	12522.62	11993.36	5208.71
GF_MN_2	5525.00	12522.62	11974.61	1451.42
CF_ST_MN_2.5	10576.60	12522.62	12283.99	10813.32
CF_ST_MN_2	7213.40	12522.62	12380.86	10309.61
GF_ST_MN_2	9576.75	12522.62	12362.11	10148.28

Two equations were used to predict the shear strength of the concrete beams: ACI – 318 Equation (16) and ACI – 318 Equation (17). Equation (16) had the same analytical shear strength of 12.5 kips for all the beams without any stirrups, since it depends only on the compressive strength of the concrete used. Equation (17) had different analytical shear strength values for FRP-only 11.9 kips and for hybrid 12.3 kips as shown in the Table 5.14. Using Canadian Educational Module Code shear force and experimental data, beam CF_St_MN_2.5 under shear-to-depth ratio of 2.5 has the highest shear force. In Figure 5.11 experimental result shows that beam GF_MN_2 has the lowest shear force and that is due to premature failure of the concrete beam.

Figure 5.12 shows the actual and experimental shear strength and force of the reinforced concrete beams.

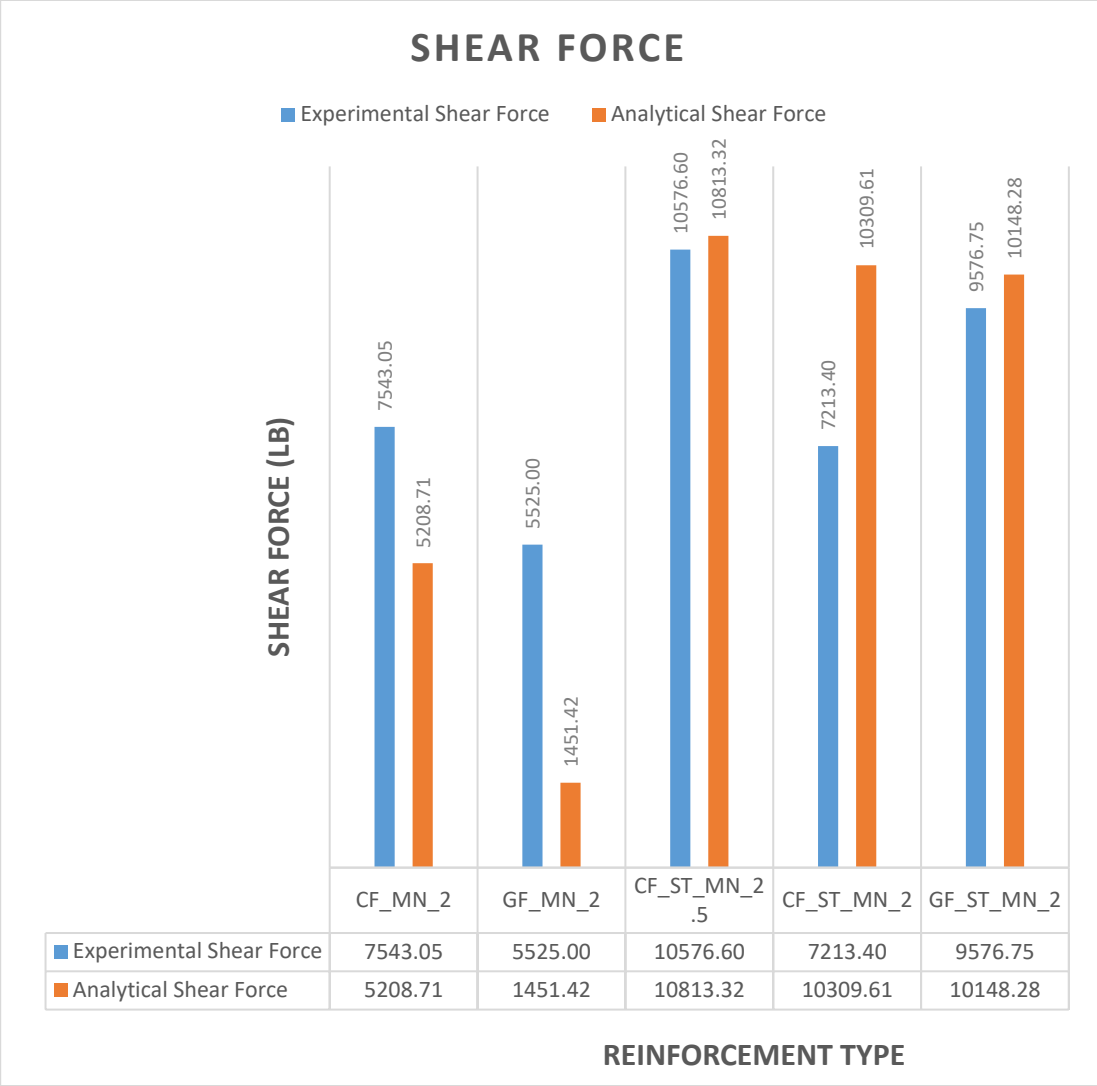

Figure 5.11: Analytical and experimental shear force

ACI Equations (19) and (20) were used to predict the shear forces. ACI equations over-predicted the shear forces of hybrid beams while under-predicting the shear force of beams reinforced with FRP-only reinforced beams. Concrete beams reinforced with hybrid reinforcement have higher shear force relative to concrete beams reinforced with FRP-only reinforcements. Hybrid CFRP grid and steel reinforced beams under shear span-to-depth ratio of 2.5 have the highest shear force relative to other beams while GFRP has the lowest.

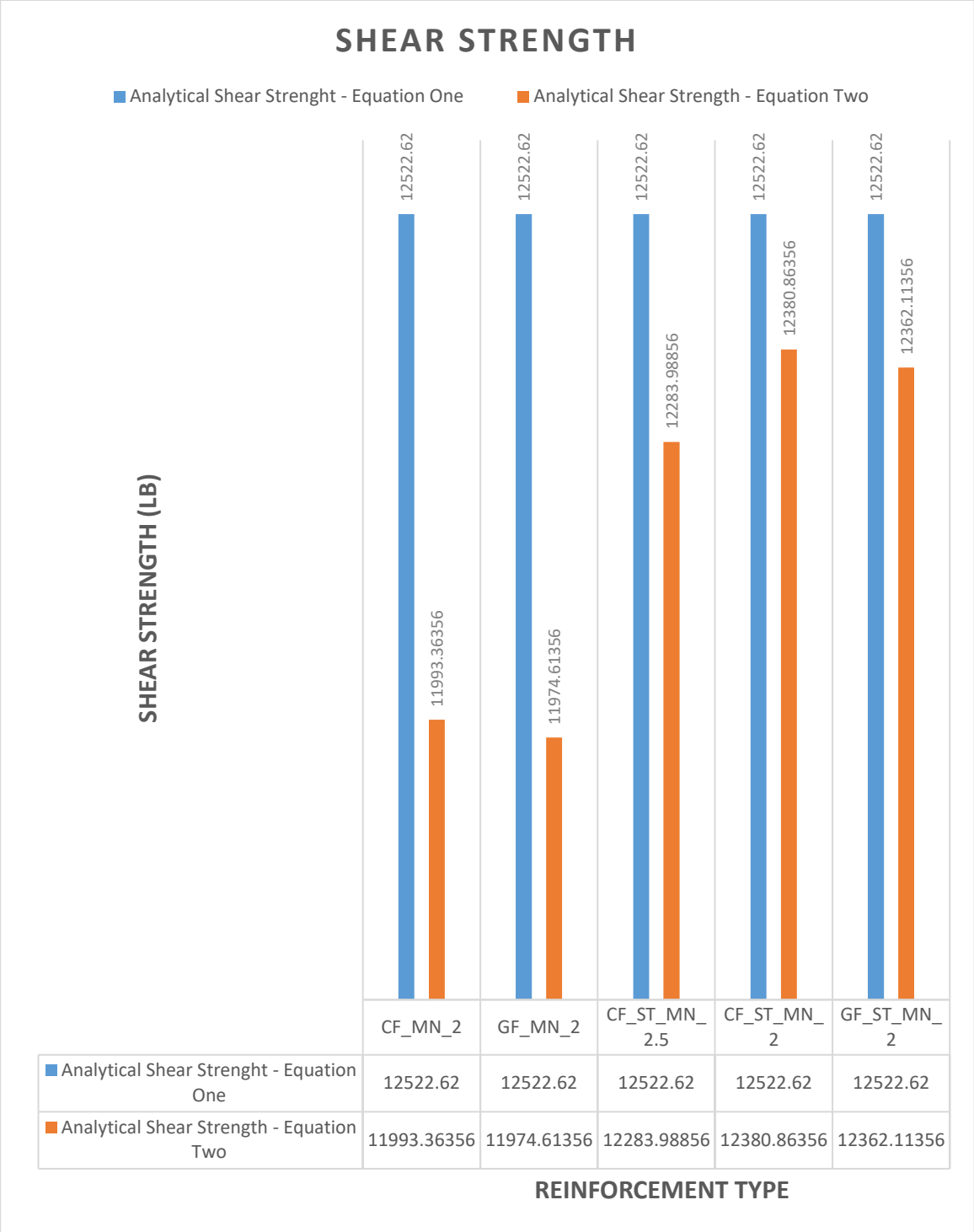

Figure 5.12: Analytical and experimental Shear Strength

Thus, the ACI Equations (16) and (17) used to predict the shear strength can accurately predict the shear strength of the concrete beam. Hybrid reinforced beams have higher shear strength compared to the beams reinforced with FRP-only.

5.5 Effective Moment of Inertia

The moment of inertia is a geometrical property of a beam cross section, which measures the beams ability to resist bending; the larger the moment of inertia the less the beam will bend. The value of effective moment of inertia (I_e) was obtained using Canadian Educational Module Code Equation (2). Equation 2 was developed for beams reinforced with FRP bars.

$$I_e = \frac{I_t I_{cr}}{I_{cr} + (1 - 0.5\left(\frac{M_{cr}}{M_a}\right)^2)(I_t - I_{cr})} \quad (20)$$

Where:

I_t = Moment of inertia at transformed section

I_{cr} = Moment of inertia of the cracked section transformed to concrete with concrete in tension is ignored

M_{cr} = Cracking moment of cross section

M_a = Maximum moment in a member of at the load stage at which deflection is being calculated.

I_t is calculated using the equation below:

$$I_t = \frac{bh\text{^}2}{12} \quad (21)$$

Where:

b = width of the concrete

h = overall member depth

All the reinforced concrete members have the same dimensions; therefore, I_t for all specimens would be the same.

Moment of inertia (I_t) = 72

I_{cr} is calculated using an equation taken from Canadian Educational Module Code, shown below:

$$I_{cr} = \frac{b(kd)^2}{3} + n_{frp\ or\ steel} A_{frp\ or\ steel} d(1-k)^2 \quad (2$$

Where:

k = Neutral axis factor or ratio of the position of the neutral axis to the effective depth used in linear elastic stress analysis

n = Modular ratio

The values of b, d, and A are already determined. To calculate the values of $n_{frp\ or\ steel}$ and k using the following equations:

$$n_{frp\ or\ steel} = \frac{E_{frp\ or\ steel}}{E_c} \quad (23$$

Table 5.15 shows the $n_{frp\ or\ steel}$ of reinforced concrete beams.

Table 5.15: Modular ratio of reinforced concrete beam

Reinforcement Type	n (Modular Ratio)
CF_MN_2	0.0079
GF_MN_2	0.0071
CF_ST_MN_2.5	0.0091
CF_ST_MN_2	0.0091
GF_ST_MN_2	0.0070

$$k = \sqrt{(\rho_{frp\ or\ steel}\, n_{frp\ or\ steel})^2 + 2\rho_{frp\ or\ steel}\, n_{frp\ or\ steel}} - \rho_{frp\ or\ steel}\, n_{frp\ or\ steel} \quad (24)$$

Table 5.16 shows the value of k using Canadian Educational Module Code Equation (24):

Table 5.16: Neutral Axis Factor or Ratio of the position of neutral axis

Reinforcement Type	k
CF_MN_2	0.112
GF_MN_2	0.056
CF_ST_MN_2.5	0.367
CF_ST_MN_2	0.367
GF_ST_MN_2	0.325

Based on the obtained values, the I_{cr} is shown in the Table 5.17:

Table 5.17: Moment of Inertia at cracked section

Reinforcement Type	Moment of Inertia I_{cr} Cracked Section
CF_MN_2	8.363011704
GF_MN_2	0.966258731
CF_ST_MN_2.5	162.777316
CF_ST_MN_2	167.0453805
GF_ST_MN_2	148.1982897

The value of M_a is already determined but to find the value of M_{cr}, the following Canadian Educational Module Code Equation (25) is used:

$$M_{cr} = \frac{f_r I_t}{y_t} \tag{25}$$

Where:

f_r = Modulus of rupture

y_t = Distance from the neutral axis to the bottom of the beam where tensile stress is maximum

$$y_t = h/2 \tag{26}$$

$$f_r = 0.6\sqrt{f'_c}\ MPa \text{ For FRP} - \text{only} \tag{27}$$

$$f_r = 0.5\sqrt{f'_c}\ MPa \text{ For Steel} - \text{only} \tag{28}$$

Using Canadian Educational Module Code and the units are in MPA, the final obtained value for f_r is multiplied by 0.15 to convert it into $^{kips}/_{in.^2}$.

$$y_t = 6$$

Table 5.18: Modulus of rupture of the reinforced concrete beams

Reinforcement Type	f_r **(kip/in2)**
CF_MN_2	0.685590913
GF_MN_2	0.685590913
CF_ST_MN_2.5	0.685590913
CF_ST_MN_2	0.685590913
GF_ST_MN_2	0.685590913

After plugging the obtained values into the equation of M_{cr}, the results are shown in the Table 5.19:

Table 5.19: Cracking Moment of reinforced concrete beam

Reinforcement Type	**M cracking (k.ft) Experimental**
CF_MN_2	0.6856
GF_MN_2	0.6856
CF_ST_MN_2.5	0.6856
CF_ST_MN_2	0.6856
GF_ST_MN_2	0.6856

The effective moment of inertia is shown in the following Table 5.20 using Canadian Educational Module Code using Equations (20):

Table 5.20: Effective moment of Inertia

Reinforcement Type	Effective Moment of Inertia (I_e)
CF_MN_2	8.367776937
GF_MN_2	0.974234385
CF_ST_MN_2.5	162.7576821
CF_ST_MN_2	167.0091219
GF_ST_MN_2	148.1716732

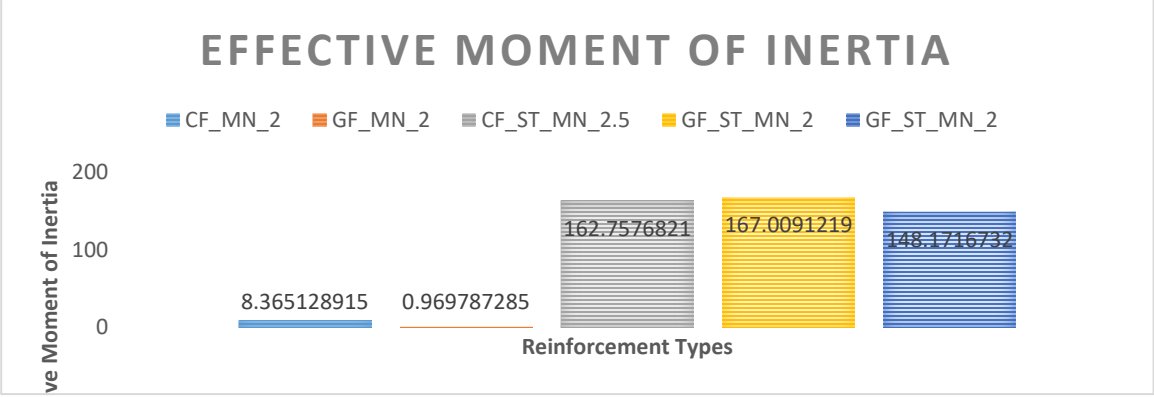

Figure 5.12: Effective Moment of Inertia of all beams

Hybrid beams have higher effective moment of inertia relative to the beams reinforced with FRP-only. The effective moment of inertia of hybrid CFRP with steel is the highest while GFRP-only reinforced beams has the lowest.

5.7 Deflection

Deflection is the movement of a reinforced concrete beam from its original position due to the forces and loads being applied. Deflection is also known as displacement which occurs due to the external load being applied [37]. In this case, static load was applied to the concrete and

the deflection was measured using LVDT. Table 5.21 shows the highest deflection in inches in each reinforced concrete beam.

Table 5.21: Actual maximum deflection in reinforced concrete beams

Reinforcement Type	Exp. Maximum Deflection (in.)
CF_MN_2	0.63
GF_MN_2	0.84
CF_ST_MN_2.5	0.32
CF_ST_MN_2	0.30
GF_ST_MN_2	0.38

In order to calculate the experimental maximum deflection in each concrete beam, the following Equation (29) from Canadian Educational Module Code is used:

$$\Delta_{Max} = \frac{Pa}{24E_c I_e}(3l^2 - 4a^2) \quad (29)$$

Where:

Δ_{Max} = Maximum Deflection

P = Maximum applied load

E_c = Effective Modulus of elasticity of concrete

I_e = Effective Moment of Inertia

l = Length of the concrete beam

Based on a previous calculation, the values of a, P, I_e and l are already determined. To find the value of E_c to obtain the experimental values of deflection, first E_c is calculated using the following equation from ACI 363:

$$E_c = 40{,}000 \left(f'_c\right)^{1/2} + 1.0\ x\ 10^6\ psi \quad (30)$$

Table 5.22 shows the obtained values of E_c:

Table 5.22: Effective modulus of elasticity of concrete

Reinforcement Type	Effective Modulus of Concrete (psi)
CF_MN_2	5380568.649
GF_MN_2	5377143.097
CF_ST_MN_2.5	5433326.256
CF_ST_MN_2	5450773.157
GF_ST_MN_2	5447401.679

Using the equation (29), the analytical maximum deflection was calculated and shown in the Table 5.24.

Table 5.23: Analytical maximum deflection of the reinforced concrete beams

Reinforcement Type	Analytical Maximum Deflection (in.)
CF_MN_2	2.75
GF_MN_2	1.11
CF_ST_MN_2.5	1.13
CF_ST_MN_2	0.91
GF_ST_MN_2	1.20

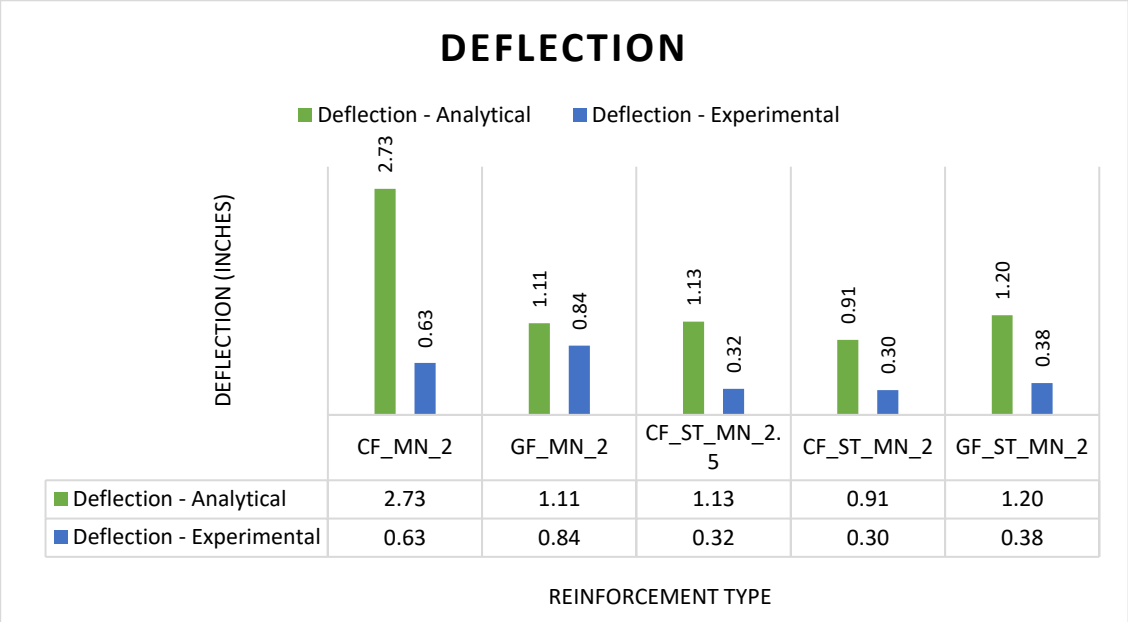

Figure 5.13: Analytical and experimental deflection of the RC beams

Figure 5.14 shows that Canadian Educational Module Code using Equation (27) over-predicted the deflection of beams reinforced with FRP-only relative to the measured values. The experimental and analytical deflection of beam CF_MN_2 is 0.63 and 2.75 inches and the experimental and analytical deflection of beam GF_MN_2 is 0.84 and 1.11 inches, which shows very poor agreement. The experimental values for hybrid FRP grid reinforced beams

are also not in good agreement to the analytical values where beam GF_ST_MN_2 has experimental and analytical deflection of 0.38 and 1.20 inches. The beam GF_ST_MN_2.5 has experimental and analytical deflection of 0.32 and 1.13 inches. Lastly CF_ST_MN_2 has the lowest deflection (0.30 inches experimental and 0.91 inches analytical).

5.6 MOMENT-CURVATURE

Moment-curvature relationship is normally used to determine the load deformation behavior of a concrete section using nonlinear material stress and strain relationship. Moment curvature is also very complex due to a large number of variables as well as nonlinear behavior involved.

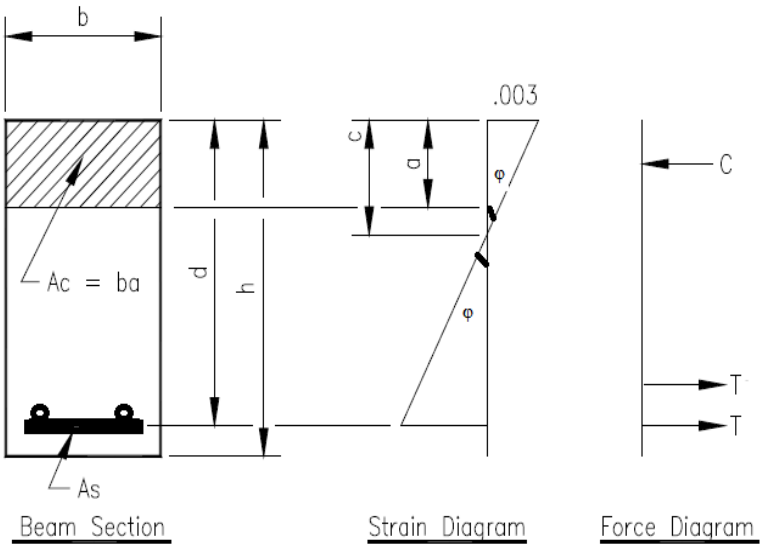

Figure 5.14: Beams Section, Strain Diagram, and Force Diagram for the RC specimens

Since the applied load was collected and the beam shear span-to-depth ratios are known, moment is calculated using Equation 28.

$$M_x = Pa \quad (31$$

Where:

M_x = Moment capacity obtained by the applied load

P = Load applied to the RC beam

a = Shear span

To calculate curvature($\emptyset$), first depth of neutral axis (c) needs to be calculated using Equation (29), then curvature can be calculated using equation (30).

$$\frac{0.003}{c} = \frac{\varepsilon_t}{d-c} \quad (32$$

$$\emptyset = \frac{\varepsilon_t}{c} \quad (33)$$

Where:

ε_t = Strain of the reinforcement collected by the strain gages

d = Effective depth of the section

$\emptyset$ = Shows the curvature of the section

The figure 5.16 shows the curvature of five reinforced specimens with hybrid and FRP-only reinforcements:

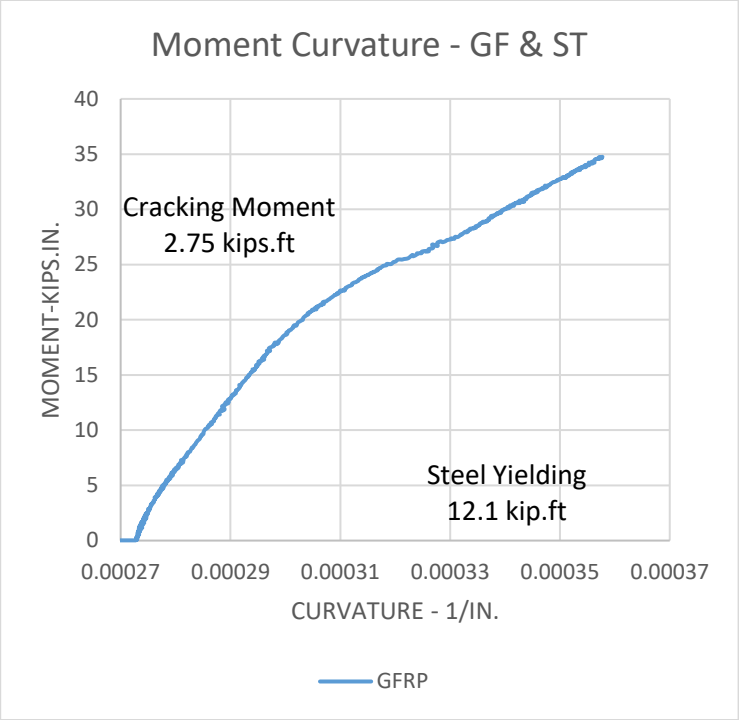

Figure 5.15: Moment Curvature of hybrid - GFRP and Steel

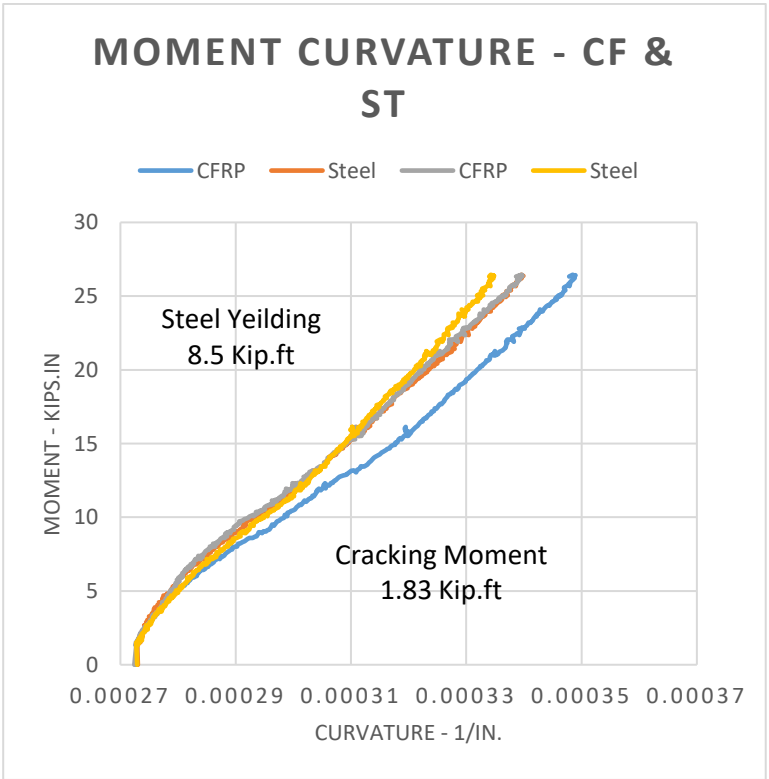

Figure 5.16: Moment Curvature of hybrid - CFRP and steel

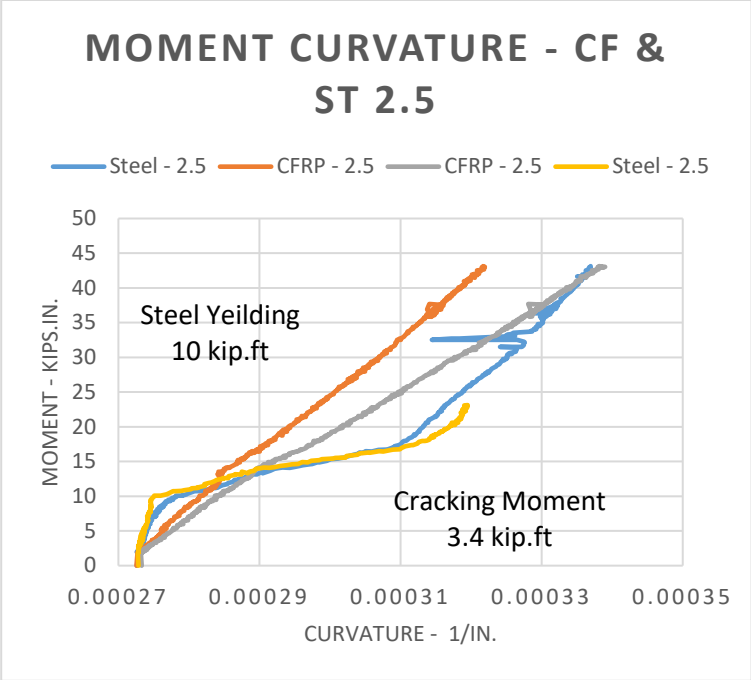

Figure 5.17: Moment Curvature of hybrid - GFRP and Steel 2.5

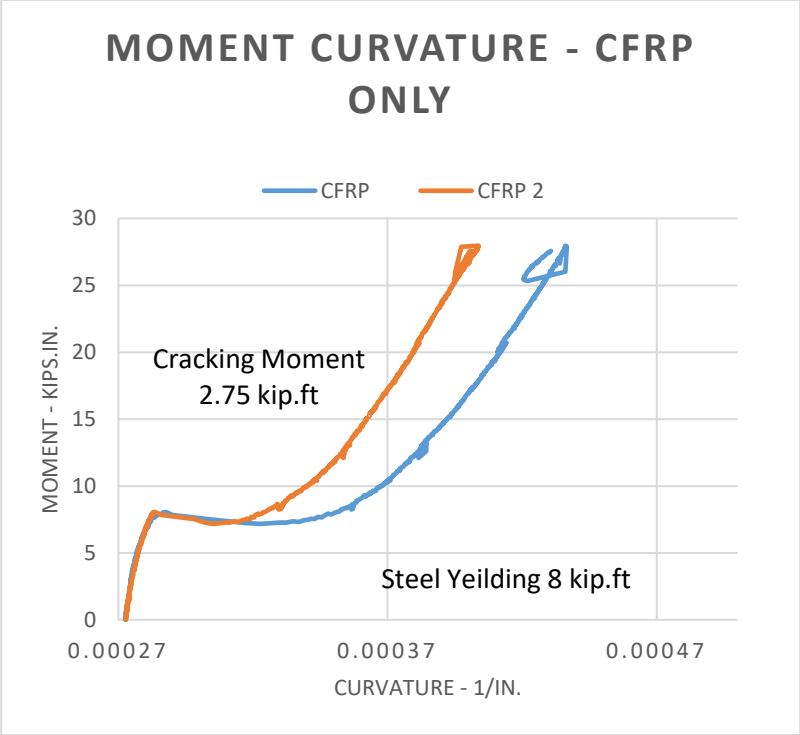

Figure 5.18: Moment Curvature of CFRP-only

Moment curvature relationship are vital for finding the ductility of the RC beams as well as the possible distribution of applied load. This relationship also demonstrates the strength, ductility, energy dissipation capacity and rigidity of sections. Figure 5.16 to 5.19 shows the moment – curvature of the 4 reinforced concrete beams. Due to the malfunction of attached strain gages and premature failure of concrete beam GF_MN_2, the moment-curvature curve was not calculated.

5.7 Beams Crack Pattern

Various crack patterns occurred when the static load was applied to the concrete beam. The cracks occur when the applied stress exceed the strength of the beam. The analytical and experimental cracking moments were calculated using Canadian Educational Module Code Equation (34) and (35):

$$M_{cr\ (predicted)} = \frac{f_{cr} I_t}{y_t} \tag{34}$$

$$M_{cr(actual)} = P_{first\ crack} a \tag{35}$$

Table 5.25 shows the experimental and analytical first cracking moment:

Table 5.24: Experimental and Analytical cracking moment

Reinforcement Type	Cracking Moment (Kip ft.) Analytical	Cracking Moment (Kip ft.) Experimental
CF_MN_2	2.75	0.46
GF_MN_2	4.125	0.46
CF_ST_MN_2.5	3.438	0.69
CF_ST_MN_2	1.83	0.69
GF_ST_MN_2	2.75	0.69

Figure 5.20 shows the crack pattern of each beam:

Table 5.25: Cracking specification of CFRP-only reinforced concrete beam

CFRP-only						
Reinforcement Type	**Experimental Failure Load (kip)**	**Analytical Failure Load (psi)**	**Experimental First Cracking Moment (kip ft.)**	**Analytical First Cracking Moment (kip ft.)**	**Failure Mode**	**First Crack load (kip)**
CF_MN_2	10.42	15.086	0.46	2.75	Shear	3

Figure 5.19: CFR- only reinforced beam after failure

Table 5.26: Cracking specification of GFRP-only reinforced concrete beam

GFRP-only						
Reinforcement Type	**Experimental Failure Load (kips)**	**Analytical Failure Load (kip)**	**Experimental Cracking Moment (kip ft.)**	**Analytical Cracking Moment**	**Failure Mode**	**First Crack load (kip)**
GF_MN_2	2.90	11.05	0.46	4.125	Shear	4.5

Figure 5.21: GFRP reinforce- only beam after failure

Table 5.27: Cracking specification of hybrid CFRP with steel reinforced concrete beam

CFRP and Steel (Hybrid) – 2.5						
Reinforcement Type	**Experimental Failure Load (kip)**	**Analytical Failure Load (kip)**	**Experimental Cracking Moment (kip ft.)**	**Analytical Cracking Moment (kip ft)**	**Failure Mode**	**First Crack load (kip)**
CF_ST_MN_2.5	21.63	21.153	0.69	3.438	Shear	3

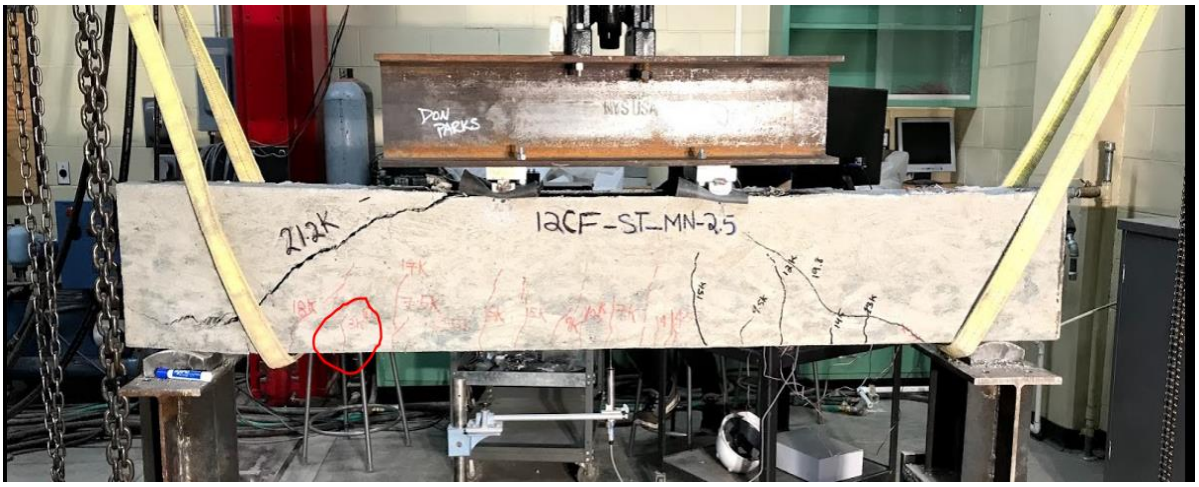

Figure 5.20: Hybrid CFRP with steel reinforced-only beam after failure

Table 5.28: Cracking specification of hybrid CFRP with steel reinforced concrete beam

CFRP and Steel (Hybrid)						
Reinforcement Type	**Experimental Failure Load (kip)**	**Analytical Failure Load (kip)**	**Experimental Cracking Moment (Kip ft.)**	**Analytical Cracking Moment (Kip ft.)**	**Failure Mode**	**First Crack load (kip)**
CF_ST_MN_2	20.62	14.4	0.69	1.83	Shear	2

Figure 5.21: Hybrid CFRP with steel reinforced-only beam after failure

Table 5.29: Cracking specification of hybrid GFRP with steel reinforced concrete beam

GFRP and Steel (Hybrid)						
Reinforcement Type	**Experimental Failure Load (kip)**	**Analytical Failure Load (kip)**	**Experimental Cracking Moment (Kip ft.)**	**Actual Cracking Moment (Kip ft.)**	**Failure Mode**	**First Crack load (kip)**
GF_ST_MN_2	20.30	19.15	0.69	2.75	Shear	3

Figure 5.22: Hybrid GFRP with steel reinforced-only beam after failure

All of the five reinforced concrete beam failed in shear. GF_MN_2 had the highest first load crack capacity while GF_ST_MN_2 had the lowest. Figure 5.20 shows the crack pattern of the beam CF_MN_2 where the first crack started at the bottom of midspan at a load of 3 kips. When the load was increased, the cracks started to propagate toward the neutral axis of the beam at different load steps until a major shear crack suddenly occurred at a load of 15 kips, when the ultimate capacity of the beam was reached. Figure 5.21 shows that GF_MN_2 was tested under monotonic load with shear span of 2 inches. The first crack occurred at the bottom middle left half of the beam under a load of 4.5. The cracks propagated in a similar way to the previous beams. The beam reached its ultimate load capacity at a load of 11 kips and a large shear crack was formed on the left side of the beam. Figure 5.22 shows that beam CF_ST_MN_2.5 with shear span of 2.5 initiated its first crack at 3 kips. Cracks started

propagating toward neutral axis until the beam failed in shear and reached its ultimate load capacity at 21.1 kips. Large shear cracks were formed on the both side of the beam. Figure 5.23 show that beam GF-ST-MN-2 initiated its first crack at 2 kips at the bottom left of the beam. Other cracks developed and propagated until the beam reach its ultimate load capacity at 14.4 kips. Lastly, figure 5.24 shows that beam GF_ST_MN_2 initiated its first crack 3 kips at the bottom of midspan. Other cracks soon propagated when the load was increased and the beam reached its ultimate load capacity at 19.1 kips. A large shear crack was formed at the left side of the beam.

CHAPTER 6: CONCLUSIONS

Fiber reinforced polymer (FRP) grids are commercially known as NEFMAC. It has been used in various applications such as bridge decks. Very limited research is available on the contribution of the FRP grids to concrete shear strength and the feasibility of using the design codes in quantifying moment capacity and shear strength of High Strength Concrete beams. This study investigates the shear behavior of High Strength Concrete beams strengthened with conventional and FRP grid together acting as a hybrid reinforcement system.

FRP reinforcements have been one of the most promising new developments for concrete structures. Structural engineers have been attempting to substitute conventional steel bars with FRP due to the following properties: corrosion-free, lightweight, easier to assemble, electromagnetic neutrality and high ratio of strength to mass ratio characteristics. In this study, six High Strength Concrete beams, each with length of 7 feet long, 12 inches thick, and 6 inches wide, were casted and tested at the University of Idaho laboratory under monotonic load with shear span-to-depth ratios of 2.0 and 2.5. Each beam was reinforced with either steel-only, CFRP/GFRP-only, or both as a hybrid reinforcement.

The following conclusions have been drawn for this study:

1. It is feasible to use CFRP and GRRP grids as reinforcements in High Strength Concrete beams to avoid any potential corrosion problems.
2. Hybrid beams indicated stable and durable shear strength compared to beams reinforced with only FRP grid and it is due to a combination of steel to the steel reinforcement.
3. Both analytical and experimental results did not show good agreement in terms of the ultimate load and maximum deflection for all beams. The load and deflection behavior

indicated that beams reinforcement with FRP-only have the largest deflection with small load. In the hybrid beams, smaller deflection with higher applied load capacity was obtained. FRP-only reinforced beams have an average 158 % and hybrid beams have an average 386% more analytical deflection relative to experimental deflection. Reinforced beam GF-ST-MN-2 have the lowest experimental (0.30 inches) and CF_MN_2 have the lowest analytical (0.91) deflection. While, CF_MN_2 has the highest analytical (2.73 inches) and GF_MN_2 has the highest experimental deflection (0.84 inches).

4. Cracks started appearing as the load capacity increases. Smalls cracks on the sides of the beam were propagated to larger and wider cracks. All of the beams failed in shear when the ultimate load capacity was reached
5. The shear span-to-depth ratio showed a negligible effect in deflection, moment capacity, crack pattern, and effective moment of inertia.
6. Both analytical and experimental results did not show good agreement in terms of the ultimate load and maximum displacement for all beams. For hybrid beams, the experimental maximum applied load was close but was not convincing. For FRP-only reinforced beams the analytical and predicted maximum applied load was different. For GF_MN_2 it was predicted that the beam had the ultimate load capacity of 2.90 kips and the experimental results indicated that the beam had the ultimate moment capacity of 11.05 kips even though this beam had premature failure.
7. Using Canadian Module Code overpredicted the deflection for hybrid and FRP-only reinforced beams with enormous margin. Analytical calculation indicated that FRP-only reinforced beams will have an average deflection of 1.9 inches while experimental data revealed an average deflection of 0.735 inches for all beams. Hybrid reinforced beams

indicated experimental average deflection of 0.33 inches while analytical deflection calculated an average deflection of 1.62 inches.

8. Hybrid beams had greater effective moment of inertia relative to FRP-only reinforced beams. The average of the effective moment of inertia for FRP-only reinforced beam was calculated 4.66 while the average effective moment of inertia for hybrid reinforced beam was predicted 159. One of the main reasons for the lower effective moment inertia of FRP beam is the premature mature failure of the GF_MN_2 and lack of shear reinforcements.
9. The modulus of rupture is not a true indicator for predicting the cracking moment and it under-predicts the cracking moment. For hybrid beams, it over-predicts the cracking moment on average by 75% relative to the actual cracking moment. For FRP-only reinforced beam, its 45%.

References

[1] Masuelli, Martin Alberto. “Introduction of Fiber-Reinforced Polymers − Polymers and Composites: Concepts, Properties and Processes.” *Introduction of Fiber-Reinforced Polymers − Polymers and Composites: Concepts, Properties and Processes InTechOpen*, Intec, 23 Jan. 2013, www.intechopen.com/books/fiber-reinforced-polymers-the-technology-applied-for-concrete-repair/introduction-of-fibre-reinforced-polymers-polymers-and-composites-concepts-properties-and-processes.

[2] “Behavior of concrete beams reinforced with hybrid steel and FRP composites.” *HBRC Journal*, Elsevier, 12 Feb. 2017, www.sciencedirect.com/science/article/pii/S1687404817300111#bb0005

[3] Jang, J., Sung, M., Han, S., Shim, W., & Yu, W. (2017, October 16). Mechanical analysis of CFRP-steel hybrid composites considering the interfacial adhesion. Retrieved November 07, 2017, from http://aip.scitation.org/doi/abs/10.1063/1.5008009

[4] Behavior of concrete beams reinforced with hybrid steel and FRP composites. (2017, February 12). Retrieved November 07, 2017, from http://www.sciencedirect.com/science/article/pii/S1687404817300111

[5] T. (2013, March 18). Five Unique Characteristics of FRP. Retrieved November 08, 2017, from http://beetleplastics.com/five-unique-characteristics-of-frp/

[6] Fang, Z., Gong, C., Yang, J., & Campbell, T. I. (2009, June 09). Nonlinear behavior of concrete beams with hybrid FRP and stainless steel reinforcements. Retrieved November 08, 2017, from https://link.springer.com/article/10.1007/s11771-009-0083-6

[7] Pang, L., Qu, W., Zhu, P., & Xu, J. (2016). Design Propositions for Hybrid FRP-Steel Reinforced Concrete Beams. *Journal of Composites for Construction, 20*(4), 04015086. doi:10.1061/(asce)cc.1943-5614.0000654

[8] Flexural behavior of hybrid FRP/steel reinforced concrete beams. (2015, April 01). Retrieved November 08, 2017, from http://www.sciencedirect.com/science/article/pii/S0263822315002664

[9] Journal of Composites for Construction. (n.d.). Retrieved November 08, 2017, from http://ascelibrary.org/doi/10.1061/%28ASCE%29CC.1943-5614.0000035

[10] Ladole, S. U. (October, 2012). Flexural Behavior of concrete beams Reinforced with Glass Fiber Polymer. *International Journal of Scientific & Engineering Research, 3*(10). doi:Prof Ram Meghan Institute of Technology & Research, Badnera,Amravati

[11] Saleh Hamed Al-sayed. (1998, July 15). Flexural behavior of concrete beams reinforced with GFRP bars. Retrieved November 08, 2017, from http://www.sciencedirect.com/science/article/pii/S0958946597000619

[12] Gross, S. P., Robert Yost, J., Dinehart, D. W., Svensen, E., & Liu, N. (n.d.). Shear Strength of Normal and High Strength Concrete Beams Reinforced with GFRP Bars. Retrieved November 08, 2017, from http://ascelibrary.org/doi/pdf/10.1061/40691%282003%2938

[13] A.F Ashour. (2005, August 29). Flexural and shear capacities of concrete beams reinforced with GFRP bars. Retrieved November 09, 2017, from http://www.sciencedirect.com/science/article/pii/S0950061805001820

[14] Tavares, D., Giongo, J., & Paultre, P. (september, 2008). Behavior of reinforced concrete beams reinforced with GFRP bars. *IBRACON Structures and Materials Journal , 1*(3), 285-295. doi:10.18411/a-2017-023

[15] Liu, Y. H., & Yuan, Y. (2012, November 29). Experimental Studies on High Strength Concrete Beams Reinforced with Steel and GFRP Rebar. Retrieved November 09, 2017, from https://www.scientific.net/AMM.238.669

[16] Alam, M. S., & Hussein, A. (2013). Size Effect on Shear Strength of FRP Reinforced Concrete Beams without Stirrups. *Journal of Composites for Construction, 17*(4), 507-516. doi:10.1061/(asce)cc.1943-5614.0000346

[17] Bentz, E. C., Massam, L., & Collins, M. P. (2010). Shear Strength of Large Concrete Members with FRP Reinforcement. *Journal of Composites for Construction, 14*(6), 637-646. doi:10.1061/(asce)cc.1943-5614.0000108

[18] Fatih Kara, I., Ashour, A. F., & Al-Paslam Koroglu, M. (2015, April 01). Flexural behavior of hybrid FRP/steel reinforced concrete beams. Retrieved November 08, 2017, from http://www.sciencedirect.com/science/article/pii/S0263822315002664

[19] Thériault, M., & Benmokrane, B. (1998). Effects of FRP Reinforcement Ratio and Concrete Strength on Flexural Behavior of Concrete Beams. *Journal of Composites for Construction, 2*(1), 7-16. doi:10.1061/(asce)1090-0268(1998)2:1(7)

[20] Leung, H., & Balendran, R. (2003). Flexural behavior of concrete beams internally reinforced with GFRP rods and steel rebar. *Structural Survey, 21*(4), 146-157. doi:10.1108/02630800310507159

[21] Correcting Concrete Corrosion. (n.d.). Retrieved November 19, 2017, from http://www.materialsperformance.com/articles/material-selection-design/2016/03/correcting-concrete-corrosion

[22] Why is reinforced concrete strong? (2017, July 06). Retrieved November 19, 2017, from http://www.explainthatstuff.com/steelconcrete.html

[23] Ultra-High Performance Concrete. (n.d.). Retrieved November 20, 2017, from http://www.cement.org/learn/concrete-technology/concrete-design-production/ultra-high-performance-concrete

[24] Basics of LVDT. (2017, July 25). Retrieved November 27, 2017, from http://www.te.com/usa-en/industries/sensor-solutions/insights/lvdt-tutorial.html

[25] Expert Logger. (n.d.). Retrieved November 27, 2017, from http://www.delphin.com/products/measuring-and-testing-devices/expert-logger.html?gclid=CjwKEAjwrIa9BRD5_dvqqazMrFESJACdv27GIjuo4SjN-hvAGNBmjN-FmDSAnG83aBtrPD5aCfWrbhoCiCnw_wcB

[26] Inc., M. (n.d.). Retrieved January 11, 2018, from http://www.moog.com/content/sites/global/en/products/actuators-servoactuators/industrial/hydraulic/test.html

[27] What is Shear Strength? - Definition from Corrosionpedia. (n.d.). Retrieved March 07, 2018, from https://www.corrosionpedia.com/definition/1026/shear-strength

[29] Isis Ec Module 3 - Notes (PDF). (n.d.). Retrieved March 07, 2018, from https://www.scribd.com/document/238594615/Isis-Ec-Module-3-Notes-PDF

[30] Deflection Definition. (n.d.). Retrieved March 15, 2018, from https://skyciv.com/tutorials/what-is-deflection/

Appendix A

Pre-Mix Inc.

PRE-MIX, INC.
6901 SR 270
PULLMAN, WA 99163
CONCRETE
(509) 872-2200
SAND & GRAVEL

UNLOADING
Free unloading time 7 1/2 minutes per cubic yard of concrete. Charge thereafter at posted truck time rates. This concrete designed in accordance with specifications indicated below

We make deliveries inside the curb line at customer's risk only and accept no responsibility whatsoever for damages resulting from such deliveries.

START REV. | FINISH REV.

LEAVE PLANT	ARRIVE JOB SITE	START DISCHARGE	FINISH DISCHARGE	ARRIVE PLANT
9:16	9:30	9:40	10:42	:

REC'D BY X

A LATE CHARGE EQUAL TO THE MAXIMUM ALLOWED BY LAW BUT NOT LESS THAN 18% ANNUAL PERCENTAGE RATE WILL BE CHARGED ON ALL PAST DUE ACCOUNTS.

THANK YOU!

ORDER NO.	CUST. NO.	PMI PRJ. NO.	CUSTOMER P.O./JOB NO.	TICKET NO.
12052	COD_CO			52351

CUSTOMER: U OF I ENGINEERING BLD — DELIVERY ADDRESS — DRIVER — DATE: 04/28/2017

DELIVERY INSTRUCTIONS

LOAD SIZE	MIX NO.	MIX DESCRIPTION	SLUMP	USE	TRUCK	SALES TAX
1.75	11844	1 SK 3/4 AGG W	3.00	BEAM	116	

LOAD QTY	DLVD QTY	ORDER QTY	PRODUCT CODE	PRODUCT DESCRIPTION	UNIT PRICE	AMOUNT
1.75	1.75	1.75	11844-1	9 SK 3/4 AGG W/WRA		
1.75	1.75	1.75	SUPER	SUPER		

TOTAL DUE

Truck 116 Driver LARRY User user Disp Ticket Num 52351 Ticket ID Time 9:05 Date 4/28/17
Load Size 1.75 yd Mix Code 11844-1 Returned Qty Mix Age 0 Seq Load ID 24512

Material	Design Qty	Required	Batched	% Var	% Moisture	Actual Wat
3/4" CUBED	1825 lb	3002 lb	3020 lb	-0.06%		gl
BLEND SAND	1450 lb	2641 lb	2640 lb	-0.03%	0.10% M	gl
TYPE I-II	848.0 lb	1480.5 lb	1480.0 lb	0.04%	4.07% A	12 gl
DARAVAIR	3.00 oz	8.25 oz	12.00 oz	-0.72%		
DARACEM	50.00 oz	87.50 oz	87.00 oz	-0.57%		
WATER	33.0 gl	45.0 gl	45.0 gl	-0.06%		
						45.0 gl

Actual Load Total: 3.00 — Mom Batches: 7531 in — Design 0.326 Water/Cement 0.322 T Manual Design 52.8 gl Trim Water 0.0 gl / load — Actual 57.7 gl To Add: 0.0 gl
Slump: 3.00 — Water in Truck: 0.0 gl Admix Water 0.0 gl / yd — 0.0 gl/ yd

ARRIVED EARLY ☐ WHEEL BARROW
ADDED WATER ☐ WAITING FOR TRUCK TO UNLOAD
JOB NOT READY ☐ LACK OF HELP
OTHER

REASON FOR DELAY

Freshly mixed cement, mortar, concrete, or grout may cause skin injury. Avoid contact with skin where possible, and wash exposed skin areas promptly with water. If any cement or cement mixture gets in the eyes, flush immediately and repeatedly with water and get prompt medical attention.

LIMITED WARRANTY

- The only liability of Pre-Mix Inc. for product defect is the return of the purchase price.
- In no event shall Pre-Mix, Inc. be liable for any direct, indirect, incidental or consequential damages resulting from the use of the products or arising out of breach of any warranty.
- All claims for damages or shortages must be made within 24 hours of delivery.

YES ☐ NO ☐ TEST CYLINDERS TAKEN

ADDITIONAL WATER ADDED TO THIS CONCRETE WILL REDUCE ITS STRENGTH

ARRIVED AT JOB WITH _____ INCH SLUMP
ADDED _____ GAL WATER AT CUSTOMER REQUEST.

CUSTOMER COPY